Mathematical Modelling and Numerical Analysis Will be set by the publisher
Modélisation Mathématique et Analyse Numérique

Submitted 26 May 2011

A STATIC CONDENSATION REDUCED BASIS ELEMENT METHOD: APPROXIMATION AND A POSTERIORI ERROR ESTIMATION

D.B.P. Huynh[1], D.J. Knezevic[2] and A.T. Patera[3]

Abstract. We propose a new reduced basis element-cum-component mode synthesis approach for parametrized elliptic coercive partial differential equations. In the Offine stage we construct a Library of interoperable parametrized reference *components* relevant to some family of problems; in the Online stage we instantiate and connect reference components (at ports) to rapidly form and query parametric *systems*. The method is based on static condensation at the interdomain level, a conforming eigenfunction "port" representation at the interface level, and finally reduced basis (RB) approximation of finite element (FE) bubble functions at the intradomain level. We show under suitable hypotheses that the RB Schur complement is close to the FE Schur complement: we can thus demonstrate the stability of the discrete equations; furthermore, we can develop inexpensive and rigorous (system-level) *a posteriori* error bounds. We present numerical results for model heat transfer and elasticity problems with particular emphasis on the Online stage; we discuss flexibility, accuracy, computational performance, and also the effectivity of the *a posteriori* error bounds.

1991 Mathematics Subject Classification. 35J25, 65N30, 65D99.

The dates will be set by the publisher.

1. Introduction

The reduced basis element (RBE) method is a computational approach for the approximation of partial differential equations which combines domain decomposition with parametric model order reduction. In particular, the "classical" RBE method typically appeals to nonconforming approaches — mortar [22] or Discontinuous Galerkin [9] — at the interdomain level and then reduced basis (RB) approximation [26] at the intradomain level. The RBE method enjoys several advantages relative to the standard "mono-domain" RB method: we are never required to solve the truth finite element (FE) problem over the full domain — we may thus address very large problems; we pursue many RB approximations over low dimensional parameter spaces rather than a single RB approximation over a very high dimensional parameter space — we may thus consider *many* parameters, as well as more general geometries and topologies. The RBE method is particularly efficient for problems which might contain many repeated subdomains as in this case a single intradomain RB preparation can be shared by all similar subdomains. Reduced basis element approximations can also be integrated with finite element approximations over regions of the domain not readily amenable to model reduction [1, 2].

In this paper we develop a static condensation RBE approach: we consider standard static condensation at the interdomain level and then RB approximation of the requisite "bubble" functions (and associated Schur complement entries) at the intradomain level. This approach extends the reach of the classical RBE in several important ways. First, in the classical RBE approach the RB spaces for a particular subdomain — which we may view as a "component" — must be aware of neighboring subdomains: components are not generally

Keywords and phrases: Reduced Basis Method, Domain Decomposition, Schur Complement, Elliptic Partial Differential Equations, *A Posteriori* Error Estimation

[1] Department of Mechanical Engineering, Massachusetts Institute of Technology, Cambridge, MA, 02139 USA; huynh@mit.edu

[2] Department of Mechanical Engineering, Massachusetts Institute of Technology, Cambridge, MA, 02139 USA; dknez@mit.edu

[3] Department of Mechanical Engineering, Massachusetts Institute of Technology, Cambridge, MA, 02139 USA; patera@mit.edu

interchangeable or interoperable and hence the analysis process is "top–down" from system to components. In contrast, in our static condensation RBE approach, the RB space for a particular component is designed to reflect all possible function variations on the component interfaces (which we shall denote "ports"): components are thus completely interchangeable and interoperable and the analysis is "bottom-up" from a library of components to many possible systems. (A similar component interchangeability is achieved in [12], based on an integral equation formulation of the RB, for electromagnetic scattering problems.) Second, in the classical mortar RBE approach, the computation of *a posteriori* error bounds necessitates appeal to the intradomain truth FE approximation in order to correct for jump terms. In contrast, in our (conforming) static condensation RBE approach, the *a posteriori* error bounds may be computed solely in terms of interface degrees of freedom and intradomain RB quantities — in essence, at very little additional cost relative to the field and output prediction.

It follows from these advantages that the static condensation RBE provides for a more favorable Offline-Online decomposition than either the standard RB method or the classical RBE approach. The Offline stage is performed once: we prepare, for each component in a library, the RB bubble spaces and colateral RB data required to populate the approximate Schur complement. The Online stage is then performed many times: we may assemble any system — we require only compatibility of ports — from multiple instantiations of components from the library; we then compute the system field and outputs, and associated *a posteriori* error bounds, for different values of the parameter in a prescribed parameter domain. The operation count and storage requirement for the Online stage depends only on the number of interface degrees of freedom and the dimension of the intradomain RB spaces. In summary, the Online stage of the static condensation RBE is much more flexible than the Online stage for the standard RB method, in which the system is already assembled and only parametric variations are permitted, and the Online stage of the classical RBE method, in which the RB intradomain spaces already reflect anticipated connectivity. The "bottom up" approach and associated Online flexibility is particularly attractive in interactive design environments, in real-time parameter estimation contexts, and more generally in discovery and optimization processes.

These advantages do of course come at some cost: increased degrees of freedom on ports (which we recall are the interfaces between the components). The RB spaces associated with the classical RBE approach reflect connectivity and thus relatively few port (Lagrange multiplier) degrees of freedom are required to ensure continuity; in contrast, in the static condensation RBE method, we must (in effect) reflect in our RB spaces any behavior of the solution over the ports. In order to minimize this parasitic effect we choose a particular interface representation (and associated lifting into the interior of the components) which (*i*) respects the relevant trace theorems and FE Schur complement theory [7] to ensure a stable discretization, (*ii*) leads to relatively economical RB spaces for the intradomain bubbles, and finally, (*iii*) permits, through a hierarchical approach, subsequent (adaptive) Online economization of port degrees of freedom. In some cases we may pursue in (*iii*) a more Draconian economization in the spirit of the classical RBE approach; indeed, in the quasi-one-dimensional limit we may even consider a single degree of freedom on each port [4].

Our approach is also closely related to the multiscale reduced basis method (MsRBM) proposed in [24]. The macroscale discretization of the MsRBM corresponds to the "system" in our static condensation RBE approach, and the microscale or subscale of the MsRBM corresponds to the "component" in the static condensation RBE approach. In the MsRBM the emphasis is thus on many macroscale elements and a very simple treatment of the macroscale–microscale interface; in contrast, in the static condensation RBE aproach, we will typically have relatively fewer components but we must include a *general* interface representation. Nevertheless, there are many similarities between the MsRBM and the static condensation RBE method, and indeed the MsRBM can perhaps take advantage of the system–level *a posteriori* error bounds developed in the current paper.

In the above we discuss the provenance of the static condensation RBE from the reduced basis perspective. However, our approach is also quite similar to the component mode synthesis (CMS) approaches which are in widespread and very effective use in industry for many years. These CMS approaches are first proposed in the seminal papers [10,16], but there is much subsequent development, refinement, and applications (see [28] for a review). As in the static condensation RBE method, the CMS approach combines static condensation at the interdomain level with model order reduction at the intradomain level. In the earlier work [10,16] the CMS model order reduction is typically of the intradomain eigenfunction modal truncation variety, however more recently Krylov spaces are also considered [15].

In our approach we directly adopt the CMS anatomy, vocabulary — components and ports — and even strategy, however we replace the intradomain modal model order reduction with RB model order reduction. This substitution can offer several advantages within the parametric context: from an approximation perspective, our approach will provide rapid convergence [5, 8, 21] over an entire parametric solution manifold; from a computational perspective, we amortize the expensive construction of the reduced order model over many system analyses (corresponding to different parameter values from the prescribed parameter domain). In short, our approach provides greater flexibility in the inexpensive Online stage: interchangeability of components is extended to include parametric variations which arise in geometry, constitutive laws, and sources and loads. Furthermore, in the static condensation RBE approach, *a posteriori* error bounds for the RB approximations at the component level permit us to develop *a posteriori* error bounds at the system level without recourse to the truth FE residual over the full domain [15]. We should note that in this paper we consider only elliptic coercive partial differential equations and not the more difficult eigenproblems or dynamic problems to which CMS approaches are typically applied.

In Section 2 we pose the symmetric coercive second-order partial differential equation for which we shall develop our approach. We also introduce the truth approximation which we wish to accelerate: a fine FE discretization defined (but, in our approach, never invoked) over the full domain. Finally, we develop the static condensation formulation of the truth FE discretization; we focus on the treatment of the interface degrees of freedom. In Section 3 we develop the static condensation RBE and we prove the well-posedness of the static condensation RBE approximation based on stability estimates developed in Brenner [7]. In Section 4 we develop the static condensation RBE system level *a posteriori* error estimates: we combine standard RB error estimates at the component level with matrix perturbation analysis [13] of the approximate Schur complement at the system level. We demonstrate that our error estimates are strict upper bounds for the actual error between the static condensation RBE approximation and the underlying truth FE discretization. In Section 5 we discuss the Offline and Online computational procedures and provide detailed operation counts and storage requirements for the Online stage in particular. Finally, in Section 6 we present numerical results for a scalar field problem (heat transfer) and a vector field problem (linear elasticity); we report the accuracy and computational cost for different representative systems and we discuss the quality of the *a posteriori* error bounds.

2. System and Component Formulations

We begin with a discussion of the system level formulation in Section 2.1. We then introduce the notions of components and ports in Section 2.2. Finally, we connect the components and system through static condensation in Section 2.3.

2.1. System Level Formulation

We introduce an abstract model problem to illustrate the system level formulation. We suppose that we are given an open domain $\Omega_{\rm SYS} \subset \mathbb{R}^d$, $d = 1, 2$ or 3, with boundary $\partial\Omega_{\rm SYS}$. We then let $X_{\rm SYS}$ denote the Hilbert space

$$X_{\rm SYS} \equiv \{v \in H^1(\Omega_{\rm SYS})\colon v|_{\partial\Omega_{{\rm SYS},D}} = 0\} \ ,$$

where $\partial\Omega_{{\rm SYS},D} \subset \partial\Omega_{\rm SYS}$ is the portion of the boundary on which we enforce Dirichlet boundary conditions. (For simplicity we consider only homogeneous Dirichlet conditions, but inhomogeneous conditions are readily treated by appropriate lifting functions.) We suppose that $X_{\rm SYS}$ is endowed with an inner product $(\cdot,\cdot)_{X,{\rm SYS}}$ and induced norm $\|\cdot\|_{X,{\rm SYS}}$. Recall that for any domain $\mathcal{O}$ in $\mathbb{R}^d$, $H^1(\mathcal{O}) \equiv \{v \in L^2(\mathcal{O})\colon \nabla v \in (L^2(\mathcal{O}))^d\}$, where $L^2(\mathcal{O}) \equiv \{v \text{ measurable over } \mathcal{O}\colon \int_{\mathcal{O}} v^2 \text{ finite}\}$.

Given a parameter $\mu \in \mathcal{D}_{\rm SYS} \subset \mathbb{R}^{P_{\rm SYS}}$, where $\mathcal{D}_{\rm SYS}$ is our compact "system parameter domain" of dimension $P_{\rm SYS}$, we look for a field $u_{\rm SYS}(\mu) \in X_{\rm SYS}$ which satisfies the weak form

$$a_{\rm SYS}(u_{\rm SYS}(\mu), v; \mu) = f_{\rm SYS}(v; \mu), \quad \forall\, v \in X_{\rm SYS} \ . \tag{1}$$

We introduce a scalar system output, $s_{\rm SYS}(\mu) \in \mathbb{R}$, given by

$$s_{\rm SYS}(\mu) \equiv \ell_{\rm SYS}(u_{\rm SYS}(\mu); \mu) \in \mathbb{R} \ . \tag{2}$$

For any $\mu \in \mathcal{D}_{\rm SYS}$, $a_{\rm SYS}(\cdot,\cdot;\mu)\colon X_{\rm SYS}\times X_{\rm SYS}\to\mathbb{R}$ is a continuous, coercive, symmetric[1] bilinear form associated with a second-order spatial partial differential operator over the system domain, $f_{\rm SYS}(\cdot;\mu)\colon X_{\rm SYS}\to\mathbb{R}$ is a continuous linear functional which represents inhomogeneities, and $\ell_{\rm SYS}(\cdot;\mu)\colon X_{\rm SYS}\to\mathbb{R}$ is a continuous linear output functional. (We do permit geometric parametrizations, but we note that $\Omega_{\rm SYS}$ is a "reference" domain and does not depend on μ; all geometry variation is accommodated by transformations to $\Omega_{\rm SYS}$ and hence appears as coefficients in $a_{\rm SYS}(\cdot,\cdot;\mu)$, $f_{\rm SYS}(\cdot;\mu)$, and $\ell_{\rm SYS}(\cdot,\mu)$.)

Let $\alpha_{\rm SYS}(\mu)$ denote the coercivity constant,

$$\alpha_{\rm SYS}(\mu) \equiv \inf_{v\in X_{\rm SYS}} \frac{a_{\rm SYS}(v,v;\mu)}{\|v\|^2_{X,{\rm SYS}}} \ . \tag{3}$$

It follows from coercivity of $a_{\rm SYS}(\cdot,\cdot;\mu)$ that there exists $\alpha_{\rm SYS,0}>0$ such that $\alpha_{\rm SYS}(\mu)>\alpha_{\rm SYS,0}$ for all $\mu\in\mathcal{D}_{\rm SYS}$. Also, let $\gamma_{\rm SYS}(\mu)$ denote the continuity constant,

$$\gamma_{\rm SYS}(\mu) \equiv \sup_{v\in X_{\rm SYS}}\sup_{w\in X_{\rm SYS}} \frac{a_{\rm SYS}(v,w;\mu)}{\|v\|_{X,{\rm SYS}}\|w\|_{X,{\rm SYS}}} \ . \tag{4}$$

It follows from continuity of $a_{\rm SYS}(\cdot,\cdot\,\mu)$ that $\gamma_{\rm SYS}(\mu)$ is finite for all $\mu\in\mathcal{D}_{\rm SYS}$.

To develop a high-fidelity approximation of $u_{\rm SYS}$, we introduce a "truth" finite element space $X^{\mathcal{N}}_{\rm SYS}\subset X_{\rm SYS}$, where $\dim(X^{\mathcal{N}}_{\rm SYS})=\mathcal{N}\gg 1$. Then, the "truth" approximation $u^{\mathcal{N}}_{\rm SYS}(\mu)\in X^{\mathcal{N}}_{\rm SYS}$ satisfies

$$a_{\rm SYS}(u^{\mathcal{N}}_{\rm SYS}(\mu),v;\mu) = f_{\rm SYS}(v;\mu), \quad \forall\, v\in X^{\mathcal{N}}_{\rm SYS} \ . \tag{5}$$

Also, the truth approximation of the output quantity, $s^{\mathcal{N}}_{\rm SYS}(\mu)$, is defined as

$$s^{\mathcal{N}}_{\rm SYS}(\mu) \equiv \ell_{\rm SYS}(u^{\mathcal{N}}_{\rm SYS}(\mu);\mu) \ . \tag{6}$$

The purpose of our RBE approximation is to provide a rapid and accurate approximation of this truth for any $\mu\in\mathcal{D}_{\rm SYS}$. We shall measure the error in the RBE approximation with respect to the truth.

2.2. **Component Level Formulation**

We now move to the component level. We suppose that the system introduced above is naturally decomposable into a set, $\mathcal{C}_{\rm SYS}$, of interconnected parametrized components. Each component COM is associated with a subdomain $\Omega_{\rm COM}$, where

$$\overline{\Omega}_{\rm SYS} = \bigcup_{{\rm COM}\in\mathcal{C}_{\rm SYS}} \overline{\Omega}_{\rm COM}, \qquad \Omega_{\rm COM}\cap\Omega_{\rm COM'}=\emptyset, \text{ for COM}\neq\text{COM}' \ .$$

For any given COM $\in\mathcal{C}_{\rm SYS}$, we let $\partial\Omega_{\rm COM}$ denote the boundary of $\Omega_{\rm COM}$, and $a_{\rm COM}(\,\cdot\,,\,\cdot\,;\mu)$ (respectively, $f_{\rm COM}(\,\cdot\,;\mu)$) denote the restriction of $a_{\rm SYS}(\,\cdot\,,\,\cdot\,;\mu)$ (respectively, $f_{\rm SYS}(\,\cdot\,;\mu)$) to $\Omega_{\rm COM}$.[2] Also, we let $(\cdot,\cdot)_{X,{\rm COM}}$ and $\|\cdot\|_{X,{\rm COM}}$ denote the restriction of the $X_{\rm SYS}$ inner product and norm to $\Omega_{\rm COM}$. (Analogous to the system level treatment of geometric parametrizations, the $\Omega_{\rm COM}$ are parameter-independent reference domains. All geometric variation is accommodated by COM-local transformations to $\Omega_{\rm COM}$ and hence appears as coefficients in the weak forms.)

Each component COM is endowed with parameters $\mu\in\mathcal{D}_{\rm COM}\subset\mathbb{R}^{P_{\rm COM}}$, and hence

$$\mathcal{D}_{\rm SYS}\subset\prod_{{\rm COM}\in\mathcal{C}_{\rm SYS}}\mathcal{D}_{\rm COM} \ .$$

[1] We note that much of the computational framework presented in this paper extends readily to non-symmetric problems, as will be discussed in future publications.

[2] The decomposition is not necessarily unique: we require only (say for a) that $a_{\rm SYS}(w,v;\mu)=\sum_{{\rm COM}\in\mathcal{C}_{\rm SYS}} a_{\rm COM}(w|_{\Omega_{\rm COM}},v|_{\rm COM};\mu)$ for any w,v in $X_{\rm SYS}$.

To minimize cumbersome notation, μ shall refer to both system and component level parameters; the precise meaning will always be evident from the context. The component parameters are related to the environment (boundary conditions and sources), material and constitutive properties, and geometry; as regards the latter, most geometric parameters are internal to the component, however some geometric parameters such as translations and rotations serve to "dock" the component compatibly within the system. Note also that topology variation is addressed at the supra-component system (assembly) level, and not within the individual components.

We now introduce a domain decomposition approach which is based upon the component structure introduced above. We begin with some notation. Recall that $\mathcal{C}_{\rm SYS}$ denotes the set of components (drawn from some given library to ensure compatibility) associated with our particular system. Each component COM $\in \mathcal{C}_{\rm SYS}$ will contain local ports — at least *one* L-P(ort) $\in \mathcal{P}_{\rm COM}$; these local ports are in turn associated to unique global ports G-P(ort) $\in \mathcal{P}^0_{\rm SYS}$. Let L-P,COM refer to a specific port in $\mathcal{P}_{\rm COM}$, and let $\Gamma_{\text{L-P,COM}}$ denote the portion of $\partial\Omega_{\rm COM}$ associated with L-P,COM. Similarly, let $\Gamma_{\text{G-P}}$ denote the domain associated with global port G-P. The mapping $\mathcal{G}$ from L-P,COM to G-P determines the particular system configuration. We suppose that $\mathcal{G}$ maps at most two distinct L-P,COM to each $\Gamma_{\text{G-P}}$ — a component has at most one neighbor on each port. Also, we assume that $\Gamma_{\text{G-P}} \cap \partial\Omega_{{\rm SYS},D}$ is either empty or $\Gamma_{\text{G-P}}$; furthermore, we define $\mathcal{P}_{\rm SYS}$ to be the set of ports $\Gamma_{\text{G-P}} \in \mathcal{P}^0_{\rm SYS}$ for which $\Gamma_{\text{G-P}} \cap \partial\Omega_{{\rm SYS},D} = \emptyset$.

For given COM $\in \mathcal{C}_{\rm SYS}$, let $X^{\mathcal{N}}_{\text{COM};0}$ denote the "component bubble space" — the restriction of $X^{\mathcal{N}}_{\rm SYS}$ to COM with homogeneous Dirichlet boundary conditions on each $\Gamma_{\text{L-P}}, \text{L-P} \in \mathcal{P}_{\rm COM}$: $X^{\mathcal{N}}_{\text{COM};0}(\Omega_{\rm COM}) \equiv \{v|_{\Omega_{\rm COM}} \colon v \in X^{\mathcal{N}}_{\rm SYS};\ v|_{\Gamma_{\text{L-P}}} = 0,\ \forall\, \text{L-P} \in \mathcal{P}_{\rm COM}\}$. Note for simplicity we suppose that triangulation over which $X^{\mathcal{N}}_{\rm SYS}$ is defined honors the domain decomposition induced by the components: $\partial\Omega_{\rm COM}$ contains only *entire* edges (on $d = 2$) or faces (on $d = 3$) of elements. Also, let $\alpha_{\rm COM}(\mu)$ denote the coercivity constant for $a_{\rm COM}$ on the space $X^{\mathcal{N}}_{\text{COM};0}$,

$$\alpha_{\rm COM}(\mu) \equiv \inf_{v \in X^{\mathcal{N}}_{\text{COM};0}} \frac{a_{\rm COM}(v, v; \mu)}{\|v\|^2_{X,\rm COM}}, \tag{7}$$

where $\alpha_{\rm COM}(\mu) \geq \alpha_{\text{COM},0} > 0,\ \forall\, \mu \in \mathcal{D}_{\rm COM}$; this coercivity property follows from the Dirichlet conditions associated with $X^{\mathcal{N}}_{\text{COM};0}$.

We express the degrees of freedom on $\Gamma_{\text{G-P}}$ in terms of an eigenfunction expansion (in $\mathbb{R}^{d-1}$) native to the port. Let $X^{\mathcal{N}}(\Gamma_{\text{G-P}})$ denote the space of restrictions of functions in $X^{\mathcal{N}}_{\rm SYS}$ to $\Gamma_{\text{G-P}}$ and let $n_{\text{G-P}} \equiv \dim(X^{\mathcal{N}}(\Gamma_{\text{G-P}}))$. We then introduce the complete set of eigenvectors, $\{\chi_k \in X^{\mathcal{N}}(\Gamma_{\text{G-P}}) \colon 1 \leq k \leq n_{\text{G-P}}\}$, associated with the discrete generalized eigenvalue problem

$$\int_{\Gamma_{\text{G-P}}} \nabla\chi_k \cdot \nabla v = \lambda_k \int_{\Gamma_{\text{G-P}}} \chi_k\, v, \qquad \forall\, v \in X^{\mathcal{N}}(\Gamma_{\text{G-P}}), \tag{8}$$

$$\|\chi_k\|_{L^2(\Gamma_{\text{G-P}})} = 1; \tag{9}$$

here the $\lambda_k \in \mathbb{R}$ denote real positive eigenvalues ordered such that $(\lambda_{\min} \equiv)\, \lambda_1 < \lambda_2 < \ldots < \lambda_{n_{\text{G-P}}}$. The χ_k satisfy the orthonormality property

$$(\chi_i, \chi_j)_{L^2(\Gamma_{\text{G-P}})} = \delta_{ij}, \tag{10}$$

where δ_{ij} denotes the Kronecker delta function.

The port eigenmodes are then elliptically lifted to the interior of neighboring components. We shall denote these lifted G-P functions $\Psi_{k,\text{G-P}}$, and we let $\omega_{\text{G-P}}$ denote the "patch" of components over which $\Psi_{k,\text{G-P}}$ has support. Also, the restriction of $\Psi_{k,\text{G-P}}$ to a constituent component COM $\in \omega_{\text{G-P}}$ shall be denoted $\psi_{k,\text{L-P,COM}}$. We construct $\psi_{k,\text{L-P,COM}}$ such that it satisfies the Laplace equation on the component interior, coincides with χ_k on $\Gamma_{\text{L-P,COM}}$, and vanishes on the remaining ports,

$$\int_{\Omega_{\rm COM}} \nabla\psi_{k,\text{L-P,COM}} \cdot \nabla v = 0, \qquad \forall\, v \in X^{\mathcal{N}}_{\text{COM};0}, \tag{11}$$

$$\psi_{k,\text{L-P,COM}} = \chi_k, \qquad \text{on } \Gamma_{\text{L-P,COM}}, \tag{12}$$

$$\psi_{k,\text{L-P,COM}} = 0, \qquad \text{on } \Gamma_{\text{L-P}',\rm COM},\ \text{L-P}' \in \mathcal{P}_{\rm COM} \setminus \text{L-P}. \tag{13}$$

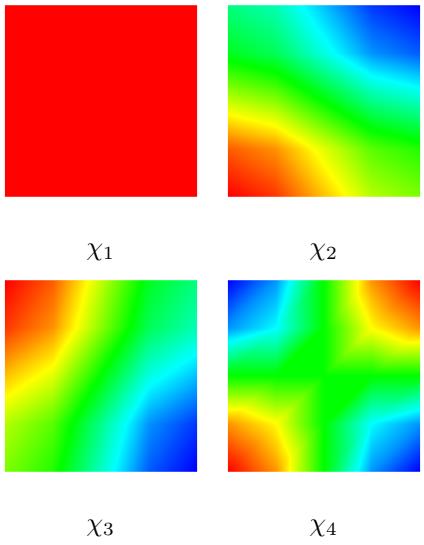

FIGURE 1. The first four modes of the eigenproblem (8),(9) for a square port $(0, 0.4)^2$ with a uniform 4×4 Q1 ($d = 2$) mesh.

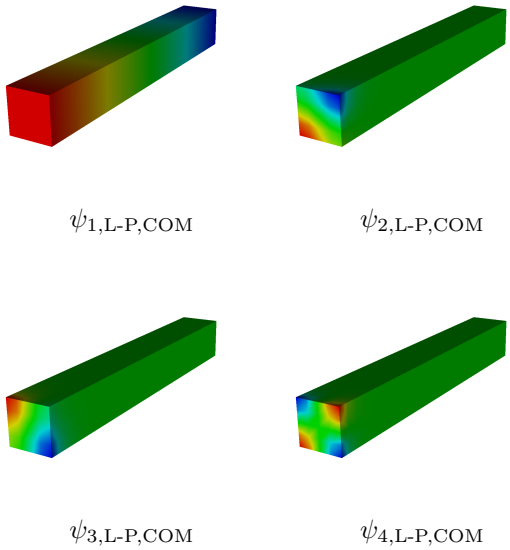

FIGURE 2. The elliptically lifted interface functions (11)–(13) corresponding to the modes in Figure 1 on a "stem" component $(0, 0.4)^2 \times (0, 3)$ with two square ports.

In (13), L-P$' \in \mathcal{P}_{\text{COM}} \setminus$ L-P refers to the set of all ports of COM except L-P. We have employed the Laplacian in (11), but of course other inner products are also possible.

For purposes of illustration we consider a component $\Omega_{\text{COM}} \equiv (0, 0.4) \times (0, 0.4) \times (0, 3)$ meshed with $4 \times 4 \times 30$ Q_1 ($d = 3$) elements; the component has two square ports, $\Gamma_{1,\text{COM}} \equiv (0, 0.4) \times (0, 0.4) \times \{0\}$ and $\Gamma_{2,\text{COM}} \equiv (0, 0.4) \times (0, 0.4) \times \{3\}$, perforce each meshed with uniform 4×4 $Q1$ ($d = 2$) elements. Figure 1 presents the first four eigenmodes for $\Gamma_{1,\text{COM}}$; Figure 2 shows the result of lifting these four port eigenmodes to the interior of the parallelepiped component.

2.3. Static Condensation

We now discuss the static condensation procedure that we employ to eliminate the degrees of freedom internal to each component. First, it is clear that we can express $u^{\mathcal{N}}_{\text{SYS}}(\mu)$ in terms of bubble and interface contributions as

$$u^{\mathcal{N}}_{\text{SYS}}(\mu) = \sum_{\text{COM} \in \mathcal{C}_{\text{SYS}}} b^{\mathcal{N}}_{\text{COM}}(\mu) + \sum_{\text{G-P} \in \mathcal{P}_{\text{SYS}}} \sum_{k=1}^{n_{\text{G-P}}} U_{k,\text{G-P}}(\mu)\, \Psi_{k,\text{G-P}} \ , \tag{14}$$

where $b^{\mathcal{N}}_{\text{COM}}(\mu) \in X^{\mathcal{N}}_{\text{COM};0}$ for each COM $\in \mathcal{C}_{\text{SYS}}$, and the $U_{k,\text{G-P}}(\mu)$, $1 \le k \le n_{\text{G-P}}$, G-P $\in \mathcal{P}_{\text{SYS}}$, are interface function coefficients. Here we implicitly assume that functions in $X^{\mathcal{N}}_{\text{COM};0}$ are extended by zero over $\Omega_{\text{SYS}} \setminus \Omega_{\text{COM}}$, and we assume an analogous extension for the $\Psi_{k,\text{G-P}}$ outside the patch $\omega_{\text{G-P}}$.

Now, since functions in $X^{\mathcal{N}}_{\text{COM};0}$ and $X^{\mathcal{N}}_{\text{COM}';0}$ do not share support, we can eliminate bubble functions from (5) in favor of global port degrees of freedom. To wit, we substitute (14) into (5) and test on the COM bubble space to obtain,

$$a_{\text{COM}}\left(b^{\mathcal{N}}_{\text{COM}}(\mu) + \sum_{\text{L-P} \in \mathcal{P}_{\text{COM}}} \sum_{k=1}^{n_{\mathcal{G}(\text{L-P,COM})}} U_{k,\mathcal{G}(\text{L-P,COM})}(\mu)\, \psi_{k,\text{L-P,COM}}, v; \mu\right) = f_{\text{COM}}(v; \mu), \quad \forall\, v \in X^{\mathcal{N}}_{\text{COM};0} \ . \tag{15}$$

It follows that $b^{\mathcal{N}}_{\rm COM}(\mu) \in X^{\mathcal{N}}_{\rm COM;0}$ satisfies,

$$a_{\rm COM}\big(b^{\mathcal{N}}_{\rm COM}(\mu), v; \mu\big) =$$

$$f_{\rm COM}(v;\mu) - \sum_{\text{L-P}\in\mathcal{P}_{\rm COM}} \sum_{k=1}^{n_{\mathcal{G}(\text{L-P,COM})}} U_{k,\mathcal{G}(\text{L-P,COM})}(\mu)\, a_{\rm COM}(\psi_{k,\text{L-P,COM}}, v; \mu), \quad \forall\, v \in X^{\mathcal{N}}_{\rm COM;0}\ , \tag{16}$$

for each COM in $\mathcal{C}_{\rm SYS}$. The existence and uniqueness of $b^{\mathcal{N}}_{\rm COM}(\mu)$ from (16) is guaranteed due to coercivity (and continuity) of $a_{\rm COM}(\,\cdot\,,\,\cdot\,;\mu)$ on $X^{\mathcal{N}}_{\rm COM;0}$.

From (16) and linearity, we can reconstruct $b^{\mathcal{N}}_{\rm COM}(\mu)$ as

$$b^{\mathcal{N}}_{\rm COM}(\mu) = b^{\mathcal{N}}_{f,\rm COM}(\mu) + \sum_{\text{L-P}\in\mathcal{P}_{\rm COM}} \sum_{k=1}^{n_{\mathcal{G}(\text{L-P,COM})}} U_{k,\mathcal{G}(\text{L-P,COM})}(\mu)\, b^{\mathcal{N}}_{k,\text{L-P,COM}}(\mu)\ , \tag{17}$$

where $b^{\mathcal{N}}_{f,\rm COM}(\mu) \in X^{\mathcal{N}}_{\rm COM;0}$ satisfies

$$a_{\rm COM}(b^{\mathcal{N}}_{f,\rm COM}(\mu), v; \mu) = f_{\rm COM}(v;\mu), \quad \forall\, v \in X^{\mathcal{N}}_{\rm COM;0}\ , \tag{18}$$

and the $b^{\mathcal{N}}_{k,\text{L-P,COM}}(\mu) \in X^{\mathcal{N}}_{\rm COM;0}$ are defined by the set of $n_{\rm COM} \equiv \sum_{\text{L-P}\in\mathcal{P}_{\rm COM}} n_{\mathcal{G}(\text{L-P,COM})}$ subproblems

$$a_{\rm COM}(b^{\mathcal{N}}_{k,\text{L-P,COM}}(\mu), v; \mu) = -a_{\rm COM}(\psi_{k,\text{L-P,COM}}, v; \mu), \quad \forall\, v \in X^{\mathcal{N}}_{\rm COM;0}\ . \tag{19}$$

Both (18) and (19) are well-posed again thanks to coercivity and continuity of $a_{\rm COM}$ over $X^{\mathcal{N}}_{\rm COM;0}$.

For $1 \le k \le n_{\text{G-P}}$ and each G-P $\in \mathcal{P}_{\rm SYS}$, let

$$\Phi_{k,\text{G-P}}(\mu) \equiv \Psi_{k,\text{G-P}} + \sum_{\rm COM\in\omega_{\text{G-P}}} b^{\mathcal{N}}_{k,\mathcal{G}^{-1}_{\rm COM}(\text{G-P})}(\mu)\ . \tag{20}$$

Here $\mathcal{G}^{-1}_{\rm COM}$ denotes the inverse map from G-P to L-P,COM on COM; recall that $\omega_{\text{G-P}}$ denotes the "patch" of components on which $\Psi_{k,\text{G-P}}$ has support. Also, we define the space

$$X^{\mathcal{N}}_{\mathcal{P}_{\rm SYS}}(\mu) \equiv \text{span}\{\Phi_{k,\text{G-P}}(\mu)\colon 1 \le k \le n_{\text{G-P}}, \forall\, \text{G-P} \in \mathcal{P}_{\rm SYS}\}, \tag{21}$$

and we endow $X^{\mathcal{N}}_{\mathcal{P}_{\rm SYS}}(\mu)$ with the inner product and norm,

$$(v,w)_{\mathcal{P}_{\rm SYS}} \equiv \sum_{\text{G-P}\in\mathcal{P}_{\rm SYS}} (v,w)_{L^2(\Gamma_{\text{G-P}})} \quad \text{and} \quad \|v\|_{\mathcal{P}_{\rm SYS}} \equiv \sqrt{(v,v)_{\mathcal{P}_{\rm SYS}}}\ , \tag{22}$$

for any $v, w \in X^{\mathcal{N}}_{\mathcal{P}_{\rm SYS}}(\mu)$.

It follows from (14) that on a component COM $\in \mathcal{C}_{\rm SYS}$, $u^{\mathcal{N}}_{\rm SYS}(\mu)$ is given by

$$u^{\mathcal{N}}_{\rm SYS}(\mu)|_{\Omega_{\rm COM}} = b^{\mathcal{N}}_{\rm COM}(\mu) + \sum_{\text{L-P}\in\mathcal{P}_{\rm COM}} \sum_{k=1}^{n_{\mathcal{G}(\text{L-P,COM})}} U_{k,\mathcal{G}(\text{L-P,COM})}(\mu)\, \psi_{k,\text{L-P,COM}}. \tag{23}$$

Hence, from (17) and (23), we have

$$u^{\mathcal{N}}_{\rm SYS}(\mu)|_{\Omega_{\rm COM}} =$$

$$b^{\mathcal{N}}_{f,\rm COM}(\mu) + \sum_{\text{L-P}\in\mathcal{P}_{\rm COM}} \sum_{k=1}^{n_{\mathcal{G}(\text{L-P,COM})}} U_{k,\mathcal{G}(\text{L-P,COM})}(\mu)\, \big(b^{\mathcal{N}}_{k,\text{L-P,COM}}(\mu) + \psi_{k,\text{L-P,COM}}\big)\,. \tag{24}$$

It then follows from (24) and (20) that the global solution can be expressed as

$$u^{\mathcal{N}}_{\rm SYS}(\mu) = \sum_{\rm COM\in\mathcal{C}_{SYS}} b^{\mathcal{N}}_{f,\rm COM}(\mu) + \sum_{\text{G-P}\in\mathcal{P}_{\rm SYS}} \sum_{k=1}^{n_{\text{G-P}}} U_{k,\text{G-P}}(\mu)\, \Phi_{k,\text{G-P}}(\mu)\ . \tag{25}$$

We now insert (25) into (5) and restrict the test space to $X^{\mathcal{N}}_{\mathcal{P}_{\rm SYS}}(\mu)$ to arrive at

$$\begin{aligned}\sum_{\text{G-P}\in\mathcal{P}_{\rm SYS}} \sum_{k=1}^{n_{\text{G-P}}} U_{k,\text{G-P}}(\mu)\, a_{\rm SYS}\big(\Phi_{k,\text{G-P}}(\mu), v;\mu\big) = \\ f_{\rm SYS}(v;\mu) - \sum_{\rm COM\in\mathcal{C}_{SYS}} a_{\rm SYS}\big(b^{\mathcal{N}}_{f,\rm COM}(\mu), v;\mu\big), \quad \forall\, v\in X^{\mathcal{N}}_{\mathcal{P}_{\rm SYS}}(\mu)\ .\end{aligned} \tag{26}$$

We now proceed to identify the linear algebraic statement associated with (26).

In particular, we test in (26) on $\Phi_{k',\text{G-P}'}(\mu)$ for $1\le k'\le n_{\text{G-P}'}$, $\forall\ \text{G-P}'\in\mathcal{P}_{\rm SYS}$, to obtain the static condensation system of dimension $n_{\rm sc}\equiv\sum_{\text{G-P}\in\mathcal{P}_{\rm SYS}} n_{\text{G-P}}$,

$$\mathbb{A}(\mu)\,\mathbb{U}(\mu) = \mathbb{F}(\mu)\ , \tag{27}$$

for the vector $\mathbb{U}(\mu)\in\mathbb{R}^{n_{\rm sc}}$ of coefficients $U_{k,\text{G-P}}(\mu)$. We may also express our system output (6) as

$$s^{\mathcal{N}}_{\rm SYS}(\mu) \equiv \big(\mathbb{L}^1(\mu)+\mathbb{L}^2(\mu)\big)^{\rm T}\,\mathbb{U}(\mu) + \sum_{\rm COM\in\mathcal{C}_{SYS}} \ell_{\rm SYS}\big(b^{\mathcal{N}}_{f,\rm COM}(\mu);\mu\big)\ .$$

We now define these static condensation quantities more explicitly.

The matrix $\mathbb{A}(\mu)\in\mathbb{R}^{n_{\rm sc}\times n_{\rm sc}}$ and vector $\mathbb{F}(\mu)\in\mathbb{R}^{n_{\rm sc}}$ are defined as

$$\mathbb{A}_{(k',\text{G-P}'),(k,\text{G-P})}(\mu) \equiv a_{\rm SYS}\big(\Phi_{k,\text{G-P}}(\mu), \Phi_{k',\text{G-P}'}(\mu);\mu\big)\ , \tag{28}$$

and

$$\mathbb{F}_{k',\text{G-P}'}(\mu) \equiv f_{\rm SYS}\big(\Phi_{k',\text{G-P}'}(\mu);\mu\big) - \sum_{\rm COM\in\mathcal{C}_{SYS}} a_{\rm SYS}\big(b^{\mathcal{N}}_{f,\rm COM}(\mu), \Phi_{k',\text{G-P}'}(\mu);\mu\big)\ , \tag{29}$$

respectively, for $1\le k\le n_{\text{G-P}}$, $\forall\ \text{G-P}\in\mathcal{P}_{\rm SYS}$, and $1\le k'\le n_{\text{G-P}'}$, $\forall\ \text{G-P}'\in\mathcal{P}_{\rm SYS}$; from (28) it is clear that $\mathbb{A}(\mu)$ is symmetric. The output vectors $\mathbb{L}^1(\mu)\in\mathbb{R}^{n_{\rm sc}}$ and $\mathbb{L}^2(\mu)\in\mathbb{R}^{n_{\rm sc}}$ are given by

$$\mathbb{L}^1_{k,\text{G-P}}(\mu) \equiv \ell_{\rm SYS}(\Psi_{k,\text{G-P}}(\mu);\mu), \quad \mathbb{L}^2_{k,\text{G-P}}(\mu) \equiv \sum_{\rm COM\in\omega_{G\text{-}P}} \ell_{\rm SYS}\Big(b^{\mathcal{N}}_{k,\mathcal{G}^{-1}_{\rm COM}(\text{G-P})}(\mu)\Big)\ , \tag{30}$$

for $1\le k\le n_{\text{G-P}}$, $\forall\ \text{G-P}\in\mathcal{P}_{\rm SYS}$. To better understand the matrices and vectors $\mathbb{A}(\mu)$ and $\mathbb{F}(\mu)$ (a similar procedure applies to $\mathbb{L}^1,\mathbb{L}^2$) we consider the assembly of the static condensation system; this assembly process, similar to finite element assembly or "stamping," is crucial to the general implementation of our approach.

Let $\mathbb{A}^{\rm COM}(\mu)\in\mathbb{R}^{m_{\rm COM}\times m_{\rm COM}}$ and $\mathbb{F}^{\rm COM}(\mu)\in\mathbb{R}^{m_{\rm COM}}$ denote the "local stiffness matrix" and "local load vector" on component COM, respectively, which from (20) has entries

$$\mathbb{A}^{\rm COM}_{(k',\text{L}-\text{P}'),(k,\text{L-P})}(\mu) \equiv a_{\rm COM}(\psi_{k,\text{L-P,COM}} + b^{\mathcal{N}}_{k,\text{L-P,COM}}(\mu), \psi_{k',\text{L-P}',\text{COM}} + b^{\mathcal{N}}_{k',\text{L-P}',\text{COM}}(\mu);\mu), \tag{31}$$

$$\begin{aligned}\mathbb{F}^{\rm COM}_{k',\text{L-P}'}(\mu) \equiv\ & f_{\rm COM}(\psi_{k',\text{L-P}',\text{COM}} + b^{\mathcal{N}}_{k',\text{L-P}',\text{COM}}(\mu);\mu) - \\ & a_{\rm COM}(b^{\mathcal{N}}_{f,\rm COM}(\mu), \psi_{k',\text{L-P}',\text{COM}} + b^{\mathcal{N}}_{k',\text{L-P}',\text{COM}}(\mu);\mu),\end{aligned} \tag{32}$$

for $1\le k\le n_{\mathcal{G}(\text{L-P,COM})}$, $\forall\ \text{L-P}\in\mathcal{P}_{\rm COM}$, and $1\le k'\le n_{\mathcal{G}(\text{L-P}',\text{COM})}$, $\forall\ \text{L-P}'\in\mathcal{P}_{\rm COM}$; note $m_{\rm COM}=\sum_{\text{L-P}\in\mathcal{P}_{\rm COM}} n_{\mathcal{G}(\text{L-P,COM})}$ is the number of port degrees of freedom in COM. Algorithm 1 then defines the assembly procedure by which we construct (in practice) (28),(29) from (31),(32); we employ the notation

Algorithm 1 Assembly of Truth Schur Complement System

$\mathbb{F}(\mu) = 0$, $\mathbb{A}(\mu) = 0$
for COM $\in \mathcal{C}_{\rm SYS}(\mu)$ **do**
  for L-P$'$ $\in \mathcal{P}_{\rm COM}, k' \in \{1, \ldots, n_{\mathcal{G}(\text{L-P}',\text{COM})}\}$ **do**
    $\mathbb{F}_{(k',\mathcal{G}(\text{L-P}',\text{COM}))}$ += $\mathbb{F}^{\rm COM}_{k',\text{L-P}'}(\mu)$
    for L-P $\in \mathcal{P}_{\rm COM}, k \in \{1, \ldots, n_{\mathcal{G}(\text{L-P},\text{COM})}\}$ **do**
      $\mathbb{A}_{(k',\mathcal{G}(\text{L-P}',\text{COM})),(k,\mathcal{G}(\text{L-P},\text{COM}))}$ += $\mathbb{A}^{\rm COM}_{(k',\text{L}-\text{P}'),(k,\text{L-P})}(\mu)$
    end for
  end for
end for

"A+=B" to represent an increment "$A \leftarrow A + B$." Note that in the case in which we require a Dirichlet condition on a port, Algorithm 1 needs a slight modification: once the assembly is complete, we *eliminate* the Dirichlet port degrees of freedom from the system — since Dirichlet G-P's are not included in $\mathcal{P}_{\rm SYS}$. This post-processing step is analogous to the standard procedure for elimination of Dirichlet rows and columns from a finite element stiffness matrix.

We close this section with a result which confirms well-posedness of the (square) system (27) and which will later serve to demonstrate well-posedness of our RB approximation.

Lemma 2.1. *There exists a constant $C(\Omega_{\rm SYS}) > 0$ such that the minimum eigenvalue of $\mathbb{A}(\mu)$, $\lambda_{\min}(\mu)$, satisfies $\lambda_{\min}(\mu) \geq C(\Omega_{\rm SYS})$, $\forall\, \mu \in \mathcal{D}_{\rm SYS}$.*

Proof. From Lemma 3.1 in [7] we obtain,

$$a_{\rm SYS}(v, v; \mu) \geq C(\Omega_{\rm SYS}; \mu)(v, v)_{\mathcal{P}_{\rm SYS}}, \quad \forall\, v \in X^{\mathcal{N}}_{\mathcal{P}_{\rm SYS}}(\mu)\ , \tag{33}$$

for $C(\Omega_{\rm SYS}; \mu) > 0$; since $\mathcal{D}_{\rm SYS}$ is compact, we can further conclude

$$a_{\rm SYS}(v, v; \mu) \geq C(\Omega_{\rm SYS})(v, v)_{\mathcal{P}_{\rm SYS}}, \quad \forall\, v \in X^{\mathcal{N}}_{\mathcal{P}_{\rm SYS}}(\mu),\ \forall\, \mu \in \mathcal{D}_{\rm SYS}\ , \tag{34}$$

for a constant $C(\Omega_{\rm SYS}) > 0$. Next, for any $v, w \in X^{\mathcal{N}}_{\mathcal{P}_{\rm SYS}}(\mu)$ expressed in terms of the basis $\{\Phi_{k,\text{G-P}} \colon 1 \leq k \leq n_{\text{G-P}}, \forall\, \text{G-P} \in \mathcal{P}_{\rm SYS}\}$ with coefficient vectors $\mathbb{V}, \mathbb{W} \in \mathbb{R}^{n_{\rm sc}}$, we obtain from (10)

$$(v, w)_{\mathcal{P}_{\rm SYS}} = \mathbb{W}^{\rm T}\mathbb{V}, \tag{35}$$

and from (28)

$$a(v, w; \mu) = \mathbb{W}^{\rm T}\mathbb{A}(\mu)\mathbb{V}. \tag{36}$$

Hence, from (34), (35), and (36) we obtain the Rayleigh quotient lower bound,

$$\lambda_{\min}(\mu) \equiv \min_{\mathbb{V} \in \mathbb{R}^{n_{\rm sc}}} \frac{\mathbb{V}^{\rm T}\mathbb{A}(\mu)\mathbb{V}}{\mathbb{V}^{\rm T}\mathbb{V}} = \min_{v \in X^{\mathcal{N}}_{\mathcal{P}_{\rm SYS}}} \frac{a_{\rm SYS}(v, v; \mu)}{(v, v)_{\mathcal{P}_{\rm SYS}}} \geq C(\mathcal{C}_{\rm SYS}), \tag{37}$$

from which the result follows. □

3. Static Condensation Reduced Basis Element Method

The static condensation procedure described above is of course very computationally expensive due to the many "bubble solves" required on each component. However, we now introduce a reduced basis (RB) approximation: in particular, we follow exactly the same procedure as in Section 2.3, except now we introduce RB approximations for the bubble functions $b^{\mathcal{N}}_{f,\rm COM}(\mu)$, $b^{\mathcal{N}}_{k,\text{L-P},\rm COM}(\mu)$. As we shall demonstrate, the resulting numerical approach will offer considerable computational savings.

To begin, from (18), for each COM $\in \mathcal{C}_{\rm SYS}$, we define the RB approximation $\tilde{b}_{f,\rm COM}(\mu) \in \widetilde{X}_{f,\text{COM};0}$,

$$a_{\rm COM}(\tilde{b}_{f,\rm COM}(\mu), v; \mu) = f_{\rm COM}(v; \mu), \quad \forall\, v \in \widetilde{X}_{f,\text{COM};0}\ , \tag{38}$$

where the RB space $\widetilde{X}_{f,\mathrm{COM};0}$ is constructed for each component COM from the standard Greedy algorithm [25]. Note that there is one RB bubble approximation $\tilde{b}_{f,\mathrm{COM}}(\mu)$ for each component COM. Next, from (19), for each COM $\in \mathcal{C}_{\mathrm{SYS}}$, we define the RB approximations $\tilde{b}_{k,\text{L-P,COM}}(\mu) \in \widetilde{X}_{k,\text{L-P,COM};0}$,

$$a_{\mathrm{COM}}(\tilde{b}_{k,\text{L-P,COM}}(\mu), v; \mu) = -a_{\mathrm{COM}}(\psi_{k,\text{L-P,COM}}, v; \mu), \quad \forall\, v \in \widetilde{X}_{k,\text{L-P,COM};0}, \tag{39}$$

where $\widetilde{X}_{k,\text{L-P,COM};0}$ is an RB approximation space (a *different* RB approximation space for each $\{k, \text{L-P,COM}\}$) obtained by a standard Greedy [25] procedure. The problems (38),(39) are well-posed due to our coercivity assumption. Note that thanks to our eigenfunction port representation the higher-mode (larger k) bubble functions will typically vanish rapidly into the interior of COM — as seen in Figure 2 for example — and thus in many cases these higher modes will depend relatively weakly on the parameter. Therefore we expect that for most of the bubble degrees of freedom a *small* RB space will suffice.

Next, in analogy to (20), for $1 \le k \le n_{\text{G-P}}$, and each G-P $\in \mathcal{P}_{\mathrm{SYS}}$, we define

$$\widetilde{\Phi}_{k,\text{L-P}}(\mu) \equiv \Psi_{k,\text{G-P}} + \sum_{\mathrm{COM} \in \omega_{\text{G-P}}} \tilde{b}_{k,\mathcal{G}_{\mathrm{COM}}^{-1}(\text{G-P})}(\mu)\ , \tag{40}$$

and then

$$\widetilde{X}_{\mathcal{P}_{\mathrm{SYS}}}(\mu) \equiv \mathrm{span}\{\widetilde{\Phi}_{k,\text{L-P}}(\mu) \colon 1 \le k \le n_{\text{G-P}}, \forall\, \text{G-P} \in \mathcal{P}_{\mathrm{SYS}}\}. \tag{41}$$

We endow $\widetilde{X}_{\mathcal{P}_{\mathrm{SYS}}}(\mu)$ with the same inner product and norm as $X^{\mathcal{N}}_{\mathcal{P}_{\mathrm{SYS}}}(\mu)$. From (25), (26) it is then natural to define $\tilde{u}_{\mathrm{SYS}}(\mu) \in \widetilde{X}^{\mathcal{N}}_{\mathcal{P}_{\mathrm{SYS}}}(\mu)$ as

$$\tilde{u}_{\mathrm{SYS}}(\mu) \equiv \sum_{\mathrm{COM} \in \mathcal{C}_{\mathrm{SYS}}} \tilde{b}_{f,\mathrm{COM}}(\mu) + \sum_{\text{G-P} \in \mathcal{P}_{\mathrm{SYS}}} \sum_{k=1}^{n_{\text{G-P}}} \widetilde{U}_{k,\text{G-P}}(\mu)\, \widetilde{\Phi}_{k,\text{G-P}}(\mu)\ , \tag{42}$$

where the coefficients $\widetilde{U}_{k,\text{G-P}}(\mu)$ satisfy

$$\begin{aligned} \sum_{\text{G-P} \in \mathcal{P}_{\mathrm{SYS}}} \sum_{k=1}^{n_{\text{G-P}}} \widetilde{U}_{k,\text{G-P}}(\mu)\, a_{\mathrm{SYS}}(\widetilde{\Phi}_{k,\text{G-P}}(\mu), v; \mu) = \\ f_{\mathrm{SYS}}(v; \mu) - \sum_{\mathrm{COM} \in \mathcal{C}_{\mathrm{SYS}}} a_{\mathrm{SYS}}(\tilde{b}_{f,\mathrm{COM}}(\mu), v; \mu), \quad \forall\, v \in \widetilde{X}^{\mathcal{N}}_{\mathcal{P}_{\mathrm{SYS}}}(\mu). \end{aligned} \tag{43}$$

We now identify the linear algebraic structure associated with (43).

In particular, we test in (43) on $\widetilde{\Phi}_{k',\text{G-P}'}(\mu)$ for $1 \le k' \le n_{\text{G-P}}$, $\forall$ G-P $\in \mathcal{P}_{\mathrm{SYS}}$, to obtain our "RB static condensation" system of dimension n_{sc},

$$\widetilde{\mathbb{A}}(\mu)\, \widetilde{\mathbb{U}}(\mu) = \widetilde{\mathbb{F}}(\mu), \tag{44}$$

for the vector $\widetilde{\mathbb{U}}(\mu) \in \mathbb{R}^{n_{\mathrm{sc}}}$ of coefficients $\widetilde{U}_{k,\text{G-P}}(\mu)$. Note that the RB system (44) is the *same* size as the truth system (27): *a priori*, there is no reduction of the truth port degrees of freedom. Furthermore, our RBE system output can be expressed as

$$\tilde{s}_{\mathrm{SYS}}(\mu) \equiv \left(\mathbb{L}^1(\mu) + \widetilde{\mathbb{L}}^2(\mu)\right)^{\mathrm{T}} \widetilde{\mathbb{U}}(\mu) + \sum_{\mathrm{COM} \in \mathcal{C}_{\mathrm{SYS}}} \ell_{\mathrm{SYS}}\big(\tilde{b}_{f,\mathrm{COM}}(\mu); \mu\big)\ . \tag{45}$$

We now define these RBE static condensation quantities more explicitly.

The matrix $\widetilde{\mathbb{A}}(\mu) \in \mathbb{R}^{n_{\mathrm{sc}} \times n_{\mathrm{sc}}}$ and vector $\widetilde{\mathbb{F}}(\mu) \in \mathbb{R}^{n_{\mathrm{sc}}}$ are defined as

$$\widetilde{\mathbb{A}}_{(k',\text{G-P}'),(k,\text{G-P})}(\mu) \equiv a_{\mathrm{SYS}}\big(\widetilde{\Phi}_{k,\text{G-P}}(\mu), \widetilde{\Phi}_{k',\text{G-P}'}(\mu); \mu\big), \tag{46}$$

$$\widetilde{\mathbb{F}}_{k',\text{G-P}'}(\mu) \equiv f_{\mathrm{SYS}}\big(\widetilde{\Phi}_{k',\text{G-P}'}(\mu); \mu\big) - \sum_{\mathrm{COM} \in \mathcal{C}_{\mathrm{SYS}}} a_{\mathrm{SYS}}\big(\tilde{b}_{f,\mathrm{COM}}(\mu), \widetilde{\Phi}_{k',\text{G-P}'}(\mu); \mu\big)\ , \tag{47}$$

respectively, for $1 \le k \le n_{\text{G-P}}$, $\forall$ G-P $\in \mathcal{P}_{\text{SYS}}$, and $1 \le k' \le n_{\text{G-P}'}$, $\forall$ G-P$' \in \mathcal{P}_{\text{SYS}}$; from (46) it is clear that $\widetilde{\mathbb{A}}(\mu)$ is symmetric. The output vector $\mathbb{L}^1$ is defined in (30) and the output vector $\widetilde{\mathbb{L}}^2(\mu) \in \mathbb{R}^{n_{\text{sc}}}$ is given by

$$\widetilde{\mathbb{L}}^2_{k,\text{G-P}}(\mu) \equiv \sum_{\text{COM} \in \omega_{\text{G-P}}} \ell_{\text{SYS}}\left(\tilde{b}_{k,\mathcal{G}^{-1}_{\text{COM(G-P)}}}(\mu)\right) , \tag{48}$$

for $1 \le k \le n_{\text{G-P}}$, $\forall$ G-P $\in \mathcal{P}_{\text{SYS}}$.

We now introduce the reduced basis versions of the "local stiffness matrix" and "local load vector": for each COM $\in \mathcal{C}_{\text{SYS}}$, from (40)

$$\begin{aligned}
\widetilde{\mathbb{A}}^{\text{COM}}_{(k',\text{L}-\text{P}'),(k,\text{L-P})}(\mu) &\equiv a_{\text{COM}}(\psi_{k,\text{L-P,COM}} + \tilde{b}_{k,\text{L-P,COM}}(\mu), \psi_{k',\text{L-P}',\text{COM}} + \tilde{b}_{k',\text{L-P}',\text{COM}}(\mu); \mu) , \quad (49)\\
\widetilde{\mathbb{F}}^{\text{COM}}_{k',\text{L-P}'}(\mu) &\equiv f_{\text{COM}}(\psi_{k',\text{L-P}',\text{COM}} + \tilde{b}_{k',\text{L-P}',\text{COM}}(\mu); \mu) - \\
&\quad a_{\text{COM}}(\tilde{b}^{\mathcal{N}}_{f,\text{COM}}(\mu), \psi_{k',\text{L-P}',\text{COM}} + \tilde{b}_{k',\text{L-P}',\text{COM}}(\mu); \mu) , \quad (50)
\end{aligned}$$

for $1 \le k \le n_{\mathcal{G}(\text{L-P,COM})}$, $\forall$ L-P $\in \mathcal{P}_{\text{COM}}$, and $1 \le k' \le n_{\mathcal{G}(\text{L-P}',\text{COM})}$, $\forall$ L-P$' \in \mathcal{P}_{\text{COM}}$. Algorithm 2 then defines the assembly procedure by which we construct (46),(47) from (49),(50). As in the truth case, Algorithm 2 requires minor post-processing in the case of Dirichlet boundary conditions.

Algorithm 2 Assembly of RB Schur Complement System

```
1: 𝔽̃(μ) = 0, 𝔸̃(μ) = 0
2: for COM ∈ 𝒞_SYS(μ) do
3:    for L-P′ ∈ 𝒫_COM, k′ ∈ {1, ..., n_𝒢(L-P′,COM)} do
4:       𝔽̃_(k′,𝒢(L-P′,COM)) += 𝔽̃^COM_(k′,L-P′)(μ)
5:       for L-P ∈ 𝒫_COM, k ∈ {1, ..., n_𝒢(L-P,COM)} do
6:          𝔸̃_(k′,𝒢(L-P′,COM)),(k,𝒢(L-P,COM)) += 𝔸̃^COM_(k′,L-P′),(k,L-P)(μ)
7:       end for
8:    end for
9: end for
```

We can prove well-posedness of the discrete problem in

Proposition 3.1. *If $\|\mathbb{A}(\mu) - \widetilde{\mathbb{A}}(\mu)\|_2 < \lambda_{\min}(\mu)$, then $\tilde{\lambda}_{\min}(\mu) > 0$, where $\tilde{\lambda}_{\min}(\mu)$ is the minimum eigenvalue of $\widetilde{\mathbb{A}}(\mu)$. Also, we have*

$$\|\widetilde{\mathbb{U}}(\mu)\|_2 \le \frac{\sqrt{\gamma_{\text{SYS}}(\mu)}}{\alpha_{\text{SYS}}(\mu)\sqrt{C(\Omega_{\text{SYS}})}} \|\hat{f}(\cdot;\mu)\|_{(X^{\mathcal{N}}_{\text{SYS}})'}, \tag{51}$$

where $\hat{f}(v;\mu) \equiv f_{\text{SYS}}(v;\mu) - \sum_{\text{COM} \in \mathcal{C}_{\text{SYS}}} a_{\text{SYS}}(\tilde{b}^{\mathcal{N}}_{f,\text{COM}}(\mu), v; \mu)$, and

$$\|\hat{f}(\cdot;\mu)\|_{(X^{\mathcal{N}}_{\text{SYS}})'} \equiv \sup_{v \in X^{\mathcal{N}}_{\text{SYS}}} \frac{\hat{f}(v;\mu)}{\|v\|_{X,\text{SYS}}}.$$

Here for $v \in \mathbb{R}^n$ (respectively, $A \in \mathbb{R}^{n \times n}$), $\|\cdot\|_2$ refers to the Euclidean norm $\|v\|_2 \equiv (v^{\text{T}}v)^{1/2}$ (respectively, induced norm $\|A\|_2 \equiv \sup_{v \in \mathbb{R}^n} \|Av\|_2/\|v\|_2$).

Proof. First we consider the bound for $\tilde{\lambda}_{\min}(\mu)$. We have

$$\begin{aligned}
\tilde{\lambda}_{\min}(\mu) &= \min_{\mathbb{V}\in\mathbb{R}^{n_{\rm sc}}} \frac{\mathbb{V}^{\rm T}\widetilde{\mathbb{A}}(\mu)\mathbb{V}}{\mathbb{V}^{\rm T}\mathbb{V}} \\
&= \min_{\mathbb{V}\in\mathbb{R}^{n_{\rm sc}}} \frac{\mathbb{V}^{\rm T}(\mathbb{A}(\mu)+(\widetilde{\mathbb{A}}(\mu)-\mathbb{A}(\mu)))\mathbb{V}}{\mathbb{V}^{\rm T}\mathbb{V}} \\
&\leq \min_{\mathbb{V}\in\mathbb{R}^{n_{\rm sc}}} \frac{\mathbb{V}^{\rm T}\widetilde{\mathbb{A}}(\mu)\mathbb{V}}{\mathbb{V}^{\rm T}\mathbb{V}} + \max_{\mathbb{V}\in\mathbb{R}^{n_{\rm sc}}} \left|\frac{\mathbb{V}^{\rm T}(\widetilde{\mathbb{A}}(\mu)-\mathbb{A}(\mu))\mathbb{V}}{\mathbb{V}^{\rm T}\mathbb{V}}\right|
\end{aligned}$$

and thus

$$|\lambda_{\min}(\mu)-\tilde{\lambda}_{\min}(\mu)| \leq \max_{\mathbb{V}\in\mathbb{R}^{n_{\rm sc}}} \left|\frac{\mathbb{V}^{\rm T}(\widetilde{\mathbb{A}}(\mu)-\mathbb{A}(\mu))\mathbb{V}}{\mathbb{V}^{\rm T}\mathbb{V}}\right| .$$

But

$$\begin{aligned}
\max_{\mathbb{V}\in\mathbb{R}^{n_{\rm sc}}} \left|\frac{\mathbb{V}^{\rm T}(\mathbb{A}(\mu)-\widetilde{\mathbb{A}}(\mu))\mathbb{V}}{\mathbb{V}^{\rm T}\mathbb{V}}\right| &\leq \max_{\mathbb{V}\in\mathbb{R}^{n_{\rm sc}}} \frac{\|\mathbb{V}\|_2\|(\mathbb{A}(\mu)-\widetilde{\mathbb{A}}(\mu))\mathbb{V}\|_2}{\|\mathbb{V}\|_2^2} \\
&= \max_{\mathbb{V}\in\mathbb{R}^{n_{\rm sc}}} \frac{\|(\mathbb{A}(\mu)-\widetilde{\mathbb{A}}(\mu))\mathbb{V}\|_2}{\|\mathbb{V}\|_2} \\
&= \|\mathbb{A}(\mu)-\widetilde{\mathbb{A}}(\mu)\|_2 .
\end{aligned}$$

Positivity of $\tilde{\lambda}_{\min}(\mu)$ then follows from the lower bound for $\lambda_{\min}(\mu)$ in Lemma 2.1.

Next, we consider the bound for $\|\mathbb{U}(\mu)\|_2$. Let

$$\tilde{u}_{\mathcal{P}_{\rm SYS}}(\mu) \equiv \sum_{\text{G}-\text{P}\in\mathcal{P}_{\rm SYS}} \sum_{k=1}^{n_{\text{G-P}}} \widetilde{U}_{k,\text{G-P}}(\mu)\,\widetilde{\Phi}_{k,\text{G-P}}(\mu) \in \widetilde{X}_{\mathcal{P}_{\rm SYS}}(\mu) .$$

Then from (43) we have

$$a_{\rm SYS}(\tilde{u}_{\mathcal{P}_{\rm SYS}}(\mu), v; \mu) = \hat{f}(v;\mu), \quad \forall\, v \in \widetilde{X}_{\mathcal{P}_{\rm SYS}}(\mu) . \tag{52}$$

Since $\widetilde{X}_{\mathcal{P}_{\rm SYS}}(\mu) \subset X^{\mathcal{N}}_{\rm SYS}$, it follows from coercivity that

$$\alpha_{\rm SYS}(\mu)\|\tilde{u}_{\mathcal{P}_{\rm SYS}}(\mu)\|^2_{X,\rm SYS} \leq a\big(\tilde{u}_{\mathcal{P}_{\rm SYS}}(\mu), \tilde{u}_{\mathcal{P}_{\rm SYS}}(\mu);\mu\big) = \hat{f}\big(\tilde{u}_{\mathcal{P}_{\rm SYS}}(\mu);\mu\big) \leq \|\hat{f}(\cdot;\mu)\|_{(X_{\rm SYS})'}\,\|\tilde{u}_{\mathcal{P}_{\rm SYS}}(\mu)\|_{X,\rm SYS} . \tag{53}$$

Hence, from (53) and continuity of $a_{\rm SYS}(\,\cdot\,,\,\cdot\,;\mu)$, we have

$$\big(a_{\rm SYS}(\tilde{u}_{\mathcal{P}_{\rm SYS}}(\mu), \tilde{u}_{\mathcal{P}_{\rm SYS}}(\mu);\mu)\big)^{1/2} \leq \sqrt{\gamma_{\rm SYS}(\mu)}\,\|\tilde{u}_{\mathcal{P}_{\rm SYS}}(\mu)\|_{X,\rm SYS} \leq \frac{\sqrt{\gamma_{\rm SYS}(\mu)}}{\alpha_{\rm SYS}(\mu)}\,\|\hat{f}(\cdot;\mu)\|_{(X^{\mathcal{N}}_{\rm SYS})'} . \tag{54}$$

Finally, (51) follows from (34) and (54). Note that $\|\hat{f}(\,\cdot\,;\mu)\|_{(X^{\mathcal{N}}_{\rm SYS})'}$ is finite thanks to boundedness of $f_{\rm SYS}$, continuity of $a_{\rm SYS}$, and well-posedness of (38). □

Proposition 3.1 implies that the static condensation RBE approximation is guaranteed to be well-posed in the limit that the errors in the RB bubble approximations tend to zero; the proposition furthermore establishes stability of the approximation. Further *a priori* results in particular related to convergence are difficult [5,8] and we instead pass to computable *a posteriori* bounds.

4. *A Posteriori* Error Analysis

We now develop a bound for the error in the system level approximation. Our approach exploits standard RB *a posteriori* error estimators [26] at the component level to develop a bound for $\|\mathbb{A}(\mu) - \widetilde{\mathbb{A}}(\mu)\|_2$; we then apply matrix perturbation analysis [13] at the system level to arrive at an *a posteriori* bound for $\|\mathbb{U}(\mu) - \widetilde{\mathbb{U}}(\mu)\|_2$ and $|s_{\rm SYS}(\mu) - \tilde{s}_{\rm SYS}(\mu)|$.

4.1. **Reduced Basis Preliminaries**

For $1 \le k \le n_{\mathcal{G}(\text{L-P,COM})}$, all L-P $\in \mathcal{P}_{\rm COM}$, and each COM $\in \mathcal{C}_{\rm SYS}$, the residual $r_{f,\rm COM}(\cdot;\mu)\colon X^{\mathcal{N}}_{\rm COM;0} \to \mathbb{R}$ for (38) is given by

$$r_{f,\rm COM}(v;\mu) \equiv f_{\rm COM}(v;\mu) - a_{\rm COM}\big(\tilde{b}_{f,\rm COM}(\mu), v;\mu\big), \quad \forall\, v \in X^{\mathcal{N}}_{\rm COM;0}\ ; \tag{55}$$

similarly, the residual $r_{k,\text{L-P,COM}}(\cdot;\mu)\colon X^{\mathcal{N}}_{\rm COM;0} \to \mathbb{R}$ for (39) is given by

$$r_{k,\text{L-P,COM}}(v;\mu) \equiv -a_{\rm COM}\big(\psi_{k,\text{L-P,COM}} + \tilde{b}_{k,\text{L-P,COM}}(\mu), v;\mu\big), \quad \forall\, v \in X^{\mathcal{N}}_{\rm COM;0}\ . \tag{56}$$

Let $\mathcal{R}_{f,\rm COM}(\mu)$ (respectively, $\mathcal{R}_{k,\text{L-P,COM}}(\mu)$) denote the dual norm of the residual (55) (respectively, (56)),

$$\mathcal{R}_{f,\rm COM}(\mu) \equiv \sup_{v\in X^{\mathcal{N}}_{\rm COM;0}} \frac{r_{f,\rm COM}(v;\mu)}{\|v\|_{X,\rm COM}}\ , \tag{57}$$

$$\mathcal{R}_{k,\text{L-P,COM}}(\mu) \equiv \sup_{v\in X^{\mathcal{N}}_{\rm COM;0}} \frac{r_{k,\text{L-P,COM}}(v;\mu)}{\|v\|_{X,\rm COM}}\ . \tag{58}$$

Note the dual norms are defined with respect to the truth bubble spaces, as our RBE error is defined relative to the truth FE.

The *a posteriori* error bounds for the bubble approximations may then be expressed in terms of these residuals, as demonstrated in

Lemma 4.1. *Given $\mu \in \mathcal{D}_{\rm COM}$, for $1 \le k \le n_{\mathcal{G}(\text{L-P,COM})}$, all* L-P $\in \mathcal{P}_{\rm COM}$*, and any* COM $\in \mathcal{C}_{\rm SYS}$*, we have*

$$\|b^{\mathcal{N}}_{f,\rm COM}(\mu) - \tilde{b}_{f,\rm COM}(\mu)\|_{X,\rm COM} \le \frac{\mathcal{R}_{f,\rm COM}(\mu)}{\alpha^{\rm LB}_{\rm COM}(\mu)}\ , \tag{59}$$

$$\|b^{\mathcal{N}}_{k,\text{L-P,COM}}(\mu) - \tilde{b}_{k,\text{L-P,COM}}(\mu)\|_{X,\rm COM} \le \frac{\mathcal{R}_{k,\text{L-P,COM}}(\mu)}{\alpha^{\rm LB}_{\rm COM}(\mu)}\ , \tag{60}$$

where $\alpha^{\rm LB}_{\rm COM}(\mu)$ satisfies

$$0 < \alpha^{\rm LB}_{\rm COM}(\mu) \le \alpha_{\rm COM}(\mu), \quad \forall\, \mu \in \mathcal{D}_{\rm COM}\ , \tag{61}$$

and

$$\alpha_{\rm COM}(\mu) \equiv \inf_{v\in X^{\mathcal{N}}_{\rm COM;0}} \frac{a_{\rm COM}(v,v;\mu)}{\|v\|_{X,\rm COM}}$$

is the COM *coercivity constant.*

Proof. We refer to the RB literature for the proof of this standard result (e.g. [25, 26]). □

Note that, in actual practice, we evaluate $\alpha^{\rm LB}_{\rm COM}(\mu)$ via the "min-Θ" approach [26], or by the Successive Constraint Method [17, 26].

4.2. **System Level Bounds**

We first derive bounds for the perturbation error in the statically condensed system matrix and load vector in

Lemma 4.2. *For any $\mu \in \mathcal{D}_{\text{SYS}}$, $\|\mathbb{F}(\mu) - \widetilde{\mathbb{F}}(\mu)\|_2 \le \sigma_1(\mu)$ and $\|\mathbb{A}(\mu) - \widetilde{\mathbb{A}}(\mu)\|_F \le \sigma_2(\mu)$. Here $\|\cdot\|_F$ denotes the matrix Frobenius norm and*

$$\sigma_1(\mu) \equiv \left\{ 2 \sum_{\text{COM} \in \mathcal{C}_{\text{SYS}}} (\Delta_{f,\text{COM}}(\mu))^2 \left(\sum_{\text{L-P} \in \mathcal{P}_{\text{COM}}} \sum_{k=1}^{n_{\mathcal{G}(\text{L-P,COM})}} (\Delta_{k,\text{L-P,COM}}(\mu))^2 \right) \right\}^{1/2}, \tag{62}$$

$$\sigma_2(\mu) \equiv \left\{ 2 \sum_{\text{COM} \in \mathcal{C}_{\text{SYS}}} \left(\sum_{\text{L-P} \in \mathcal{P}_{\text{COM}}} \sum_{k=1}^{n_{\mathcal{G}(\text{L-P,COM})}} (\Delta_{k,\text{L-P,COM}}(\mu))^2 \right)^2 \right\}^{1/2}, \tag{63}$$

where

$$\Delta_{f,\text{COM}}(\mu) \equiv \mathcal{R}_{f,\text{COM}}(\mu) / \sqrt{\alpha^{\text{LB}}_{\text{COM}}(\mu)}\,, \tag{64}$$

$$\Delta_{k,\text{L-P,COM}}(\mu) \equiv \mathcal{R}_{k,\text{L-P,COM}}(\mu) / \sqrt{\alpha^{\text{LB}}_{\text{COM}}(\mu)}\,, \tag{65}$$

for $\alpha^{\text{LB}}_{\text{COM}}$ satisfying (61).

Proof. The proofs for (62) and (63) are similar and we thus restrict attention to the more involved case, (63). To derive a bound for $\|\mathbb{A}(\mu) - \widetilde{\mathbb{A}}(\mu)\|_F$, we start with a component-level bound for $\|\mathbb{A}^{\text{COM}}(\mu) - \widetilde{\mathbb{A}}^{\text{COM}}(\mu)\|_F$. For the error in a single entry on a component $\text{COM} \in \mathcal{C}_{\text{SYS}}$, we have

$$\begin{aligned}
&|\mathbb{A}^{\text{COM}}_{(k',\text{L-P}'),(k,\text{L-P})}(\mu) - \widetilde{\mathbb{A}}^{\text{COM}}_{(k',\text{L-P}'),(k,\text{L-P})}(\mu)| \\
&\quad = \big| a_{\text{COM}}(\psi_{k,\text{L-P,COM}}(\mu) + b^{\mathcal{N}}_{k,\text{L-P,COM}}(\mu), \psi_{k',\text{L-P}',\text{COM}}(\mu); \mu) + b^{\mathcal{N}}_{k',\text{L-P}',\text{COM}}(\mu); \mu) \\
&\qquad - a_{\text{COM}}(\psi_{k,\text{L-P,COM}}(\mu) + \tilde{b}_{k,\text{L-P,COM}}(\mu), \psi_{k',\text{L-P}',\text{COM}}(\mu); \mu) + \tilde{b}_{k',\text{L-P}',\text{COM}}(\mu); \mu) \big| \\
&\quad = \big| a_{\text{COM}}\big(b^{\mathcal{N}}_{k,\text{L-P,COM}}(\mu), \psi_{k',\text{L-P}',\text{COM}}(\mu); \mu\big) \\
&\qquad + a_{\text{COM}}\big(\psi_{k,\text{L-P,COM}}(\mu) + b^{\mathcal{N}}_{k,\text{L-P,COM}}(\mu), b^{\mathcal{N}}_{k',\text{L-P}',\text{COM}}(\mu); \mu\big) \\
&\qquad - a_{\text{COM}}\big(\tilde{b}_{k,\text{L-P,COM}}(\mu), \psi_{k',\text{L-P}',\text{COM}}(\mu); \mu\big) \\
&\qquad - a_{\text{COM}}\big(\psi_{k,\text{L-P,COM}}(\mu) + \tilde{b}_{k,\text{L-P,COM}}(\mu), \tilde{b}_{k',\text{L-P}',\text{COM}}(\mu); \mu\big) \big|\,.
\end{aligned} \tag{66}$$

Since $b^{\mathcal{N}}_{k',\text{L-P}',\text{COM}}(\mu) \in X^{\mathcal{N}}_{\text{COM};0}$, it follows from (19) that

$$a_{\text{COM}}\big(\psi_{k,\text{L-P,COM}}(\mu) + b^{\mathcal{N}}_{k,\text{L-P,COM}}(\mu), b^{\mathcal{N}}_{k',\text{L-P}',\text{COM}}(\mu); \mu\big) = 0. \tag{67}$$

Also, from (19) and symmetry of a_{COM}, we have

$$\begin{aligned}
a_{\text{COM}}\big(b^{\mathcal{N}}_{k,\text{L-P,COM}}(\mu), \psi_{k',\text{L-P}',\text{COM}}(\mu); \mu\big) &= -a_{\text{COM}}\big(b^{\mathcal{N}}_{k,\text{L-P,COM}}(\mu), b^{\mathcal{N}}_{k',\text{L-P}',\text{COM}}(\mu); \mu\big) \\
&= a_{\text{COM}}\big(\psi_{k,\text{L-P,COM}}(\mu), b^{\mathcal{N}}_{k',\text{L-P}',\text{COM}}(\mu); \mu\big)\,,
\end{aligned} \tag{68}$$

and

$$a_{\text{COM}}\big(\tilde{b}_{k,\text{L-P,COM}}(\mu), \psi_{k',\text{L-P}',\text{COM}}(\mu); \mu\big) = -a_{\text{COM}}\big(\tilde{b}_{k,\text{L-P,COM}}(\mu), b^{\mathcal{N}}_{k',\text{L-P}',\text{COM}}(\mu); \mu\big). \tag{69}$$

Hence, (66) with (56), (67), (68), (69) implies

$$\begin{aligned}
&\left|\mathbb{A}^{\mathrm{COM}}_{(k',\text{L-P}'),(k,\text{L-P})}(\mu) - \widetilde{\mathbb{A}}^{\mathrm{COM}}_{(k',\text{L-P}'),(k,\text{L-P})}(\mu)\right| \\
&\quad = \left|a_{\mathrm{COM}}\big(\psi_{k,\text{L-P},\mathrm{COM}}(\mu) + \tilde{b}_{k,\text{L-P},\mathrm{COM}}(\mu), b^{\mathcal{N}}_{k',\text{L-P}',\mathrm{COM}}(\mu);\mu\big)\right. \\
&\qquad \left. - a_{\mathrm{COM}}\big(\psi_{k,\text{L-P},\mathrm{COM}}(\mu) + \tilde{b}_{k,\text{L-P},\mathrm{COM}}(\mu), \tilde{b}_{k',\text{L-P}',\mathrm{COM}}(\mu);\mu\big)\right| \\
&\quad = \left|a_{\mathrm{COM}}\big(\psi_{k,\text{L-P},\mathrm{COM}}(\mu) + \tilde{b}_{k,\text{L-P},\mathrm{COM}}(\mu), b^{\mathcal{N}}_{k',\text{L-P}',\mathrm{COM}}(\mu) - \tilde{b}_{k',\text{L-P}',\mathrm{COM}}(\mu);\mu\big)\right| \\
&\quad = \left|r_{k,\text{L-P},\mathrm{COM}}\big(b^{\mathcal{N}}_{k',\text{L-P}',\mathrm{COM}}(\mu) - \tilde{b}_{k',\text{L-P}',\mathrm{COM}}(\mu);\mu\big)\right| .
\end{aligned}$$

It thus follows from (58) and Lemma 4.1 that

$$\begin{aligned}
&\left|\mathbb{A}^{\mathrm{COM}}_{(k',\text{L-P}'),(k,\text{L-P})}(\mu) - \widetilde{\mathbb{A}}^{\mathrm{COM}}_{(k',\text{L-P}'),(k,\text{L-P})}(\mu)\right| \\
&\quad = \frac{\left|r_{k,\text{L-P},\mathrm{COM}}\big(b^{\mathcal{N}}_{k',\text{L-P}',\mathrm{COM}}(\mu) - \tilde{b}_{k',\text{L-P}',\mathrm{COM}}(\mu);\mu\big)\right|}{\left\|b^{\mathcal{N}}_{k',\text{L-P}',\mathrm{COM}}(\mu) - \tilde{b}_{k',\text{L-P}',\mathrm{COM}}(\mu)\right\|_{X,\mathrm{COM}}} \left\|b^{\mathcal{N}}_{k',\text{L-P}',\mathrm{COM}}(\mu) - \tilde{b}_{k',\text{L-P}',\mathrm{COM}}(\mu)\right\|_{X,\mathrm{COM}} \\
&\quad \le \mathcal{R}_{k,\text{L-P},\mathrm{COM}}(\mu) \left\|b^{\mathcal{N}}_{k',\text{L-P}',\mathrm{COM}}(\mu) - \tilde{b}_{k',\text{L-P}',\mathrm{COM}}(\mu)\right\|_{X,\mathrm{COM}} \\
&\quad \le \mathcal{R}_{k,\text{L-P},\mathrm{COM}}(\mu)\, \mathcal{R}_{k',\text{L-P}',\mathrm{COM}}(\mu)/\alpha^{\mathrm{LB}}_{\mathrm{COM}}(\mu) \\
&\quad = \Delta_{k,\text{L-P},\mathrm{COM}}(\mu)\, \Delta_{k',\text{L-P}',\mathrm{COM}}(\mu) . \qquad (70)
\end{aligned}$$

Then, a Frobenius norm bound for the error in the "local stiffness matrix" for COM is given by

$$\begin{aligned}
&\|\mathbb{A}^{\mathrm{COM}}(\mu) - \widetilde{\mathbb{A}}^{\mathrm{COM}}(\mu)\|^2_F \\
&\quad \le \sum_{\text{L-P}\in\mathcal{P}_{\mathrm{COM}}} \sum_{k=1}^{n_{\mathcal{G}(\text{L-P},\mathrm{COM})}} \sum_{\text{L-P}'\in\mathcal{P}_{\mathrm{COM}}} \sum_{k'=1}^{n_{\mathcal{G}(\text{L-P}',\mathrm{COM})}} \left(\Delta_{k,\text{L-P},\mathrm{COM}}(\mu)\, \Delta_{k',\text{L-P}',\mathrm{COM}}(\mu)\right)^2 \\
&\quad = \left(\sum_{\text{L-P}\in\mathcal{P}_{\mathrm{COM}}} \sum_{k=1}^{n_{\mathcal{G}(\text{L-P},\mathrm{COM})}} \Delta_{k,\text{L-P},\mathrm{COM}}(\mu)^2\right)\left(\sum_{\text{L-P}'\in\mathcal{P}_{\mathrm{COM}}} \sum_{k'=1}^{n_{\mathcal{G}(\text{L-P}',\mathrm{COM})}} \Delta_{k',\text{L-P}',\mathrm{COM}}(\mu)^2\right) \\
&\quad = \left(\sum_{\text{L-P}\in\mathcal{P}_{\mathrm{COM}}} \sum_{k=1}^{n_{\mathcal{G}(\text{L-P},\mathrm{COM})}} \Delta_{k,\text{L-P},\mathrm{COM}}(\mu)^2\right)^2 . \qquad (71)
\end{aligned}$$

Finally, we recall that we suppose that each entry of $\mathbb{A}(\mu)$ and $\widetilde{\mathbb{A}}(\mu)$ is assembled from a sum of terms from at most two different local stiffness matrices; thus (63) follows from (71) and the inequality $(a+b)^2 \le 2(a^2+b^2)$. □

We note that the proof of Lemma 4.2 relies on the symmetry of the $a_{\mathrm{COM}}(\cdot,\cdot;\mu)$; the proof can be generalized to the non-symmetric case with a primal-dual RB formulation [26].

We now bound the solution error in

Proposition 4.3. *If $\tilde{\lambda}_{\min}(\mu) > \sigma_1(\mu)$, then*

$$\|\mathbb{U}(\mu) - \widetilde{\mathbb{U}}(\mu)\|_2 \le \Delta\mathbb{U}(\mu) , \qquad (72)$$

where

$$\Delta\mathbb{U}(\mu) \equiv \frac{\sigma_1(\mu) + \sigma_2(\mu)\|\widetilde{\mathbb{U}}(\mu)\|_2 + \|\widetilde{\mathbb{F}}(\mu) - \widetilde{\mathbb{A}}(\mu)\widetilde{\mathbb{U}}(\mu)\|_2}{\tilde{\lambda}_{\min}(\mu) - \sigma_2(\mu)} \ . \tag{73}$$

Recall that $\|\cdot\|_2$ *refers to the Euclidean norm.*

Proof. Let $\delta\mathbb{A}(\mu) \equiv \mathbb{A}(\mu) - \widetilde{\mathbb{A}}(\mu)$, $\delta\mathbb{F}(\mu) \equiv \mathbb{F}(\mu) - \widetilde{\mathbb{F}}(\mu)$, and $\delta\mathbb{U}(\mu) = \mathbb{U}(\mu) - \widetilde{\mathbb{U}}(\mu)$. Then, from (27), we have the identity

$$[\widetilde{\mathbb{A}}(\mu) + \delta\mathbb{A}(\mu)]\ \delta\mathbb{U}(\mu) = \delta\mathbb{F}(\mu) - \delta\mathbb{A}(\mu)\ \widetilde{\mathbb{U}}(\mu) + (\widetilde{\mathbb{F}}(\mu) - \widetilde{\mathbb{A}}(\mu)\widetilde{\mathbb{U}}(\mu)) \ . \tag{74}$$

(Note if (44) is solved exactly then the last term on the right-hand side of (74) vanishes; however, we retain the term to accommodate (for example) iterative solution error.) We pre-multiply (74) by $\delta\mathbb{U}(\mu)^{\mathrm{T}}$ and divide by $\delta\mathbb{U}(\mu)^{\mathrm{T}}\ \delta\mathbb{U}(\mu)$ to obtain

$$\begin{aligned}
\tilde{\lambda}_{\min}(\mu) \ \le \ \frac{\delta\mathbb{U}(\mu)^{\mathrm{T}}\widetilde{\mathbb{A}}(\mu)\delta\mathbb{U}(\mu)}{\delta\mathbb{U}(\mu)^{\mathrm{T}}\delta\mathbb{U}(\mu)} \ &\le \ \left|\frac{\delta\mathbb{U}(\mu)^{\mathrm{T}}\delta\mathbb{F}(\mu)}{\delta\mathbb{U}(\mu)^{\mathrm{T}}\delta\mathbb{U}(\mu)}\right| + \left|\frac{\delta\mathbb{U}(\mu)^{\mathrm{T}}\delta\mathbb{A}(\mu)\widetilde{\mathbb{U}}(\mu)}{\delta\mathbb{U}(\mu)^{\mathrm{T}}\delta\mathbb{U}(\mu)}\right| \\
&\quad + \left|\frac{\delta\mathbb{U}(\mu)^{\mathrm{T}}\delta\mathbb{A}(\mu)\delta\mathbb{U}(\mu)}{\delta\mathbb{U}(\mu)^{\mathrm{T}}\delta\mathbb{U}(\mu)}\right| + \left|\frac{\delta\mathbb{U}(\mu)^{\mathrm{T}}(\widetilde{\mathbb{F}}(\mu) - \widetilde{\mathbb{A}}(\mu)\widetilde{\mathbb{U}}(\mu))}{\delta\mathbb{U}(\mu)^{\mathrm{T}}\delta\mathbb{U}(\mu)}\right| \\
&\le \ \frac{\|\delta\mathbb{F}(\mu)\|_2 + \|\delta\mathbb{A}(\mu)\ \mathbb{U}(\mu)\|_2 + \|\widetilde{\mathbb{F}}(\mu) - \widetilde{\mathbb{A}}(\mu)\widetilde{\mathbb{U}}(\mu)\|_2}{\|\delta\mathbb{U}\|_2} + \|\delta\mathbb{A}(\mu)\|_2 \qquad (75) \\
&\le \ \frac{\|\delta\mathbb{F}(\mu)\|_2 + \|\delta\mathbb{A}(\mu)\|_2\ \|\widetilde{\mathbb{U}}(\mu)\|_2 + \|\widetilde{\mathbb{F}}(\mu) - \widetilde{\mathbb{A}}(\mu)\widetilde{\mathbb{U}}(\mu)\|_2}{\|\delta\mathbb{U}(\mu)\|_2} + \|\delta\mathbb{A}(\mu)\|_2 \\
&\le \ \frac{\sigma_1(\mu) + \sigma_2(\mu)\ \|\widetilde{\mathbb{U}}(\mu)\|_2 + \|\widetilde{\mathbb{F}}(\mu) - \widetilde{\mathbb{A}}(\mu)\widetilde{\mathbb{U}}(\mu)\|_2}{\|\delta\mathbb{U}(\mu)\|_2} + \sigma_2(\mu), \qquad (76)
\end{aligned}$$

where we have employed the bound $\|\delta\mathbb{A}(\mu)\|_2 \le \|\delta\mathbb{A}(\mu)\|_F \le \sigma_2(\mu)$ (recall that $\|\cdot\|_2 \le \|\cdot\|_F$ is a consequence of the Cauchy-Schwarz inequality). The desired result (72),(73) then follows straightforwardly from (76). □

It is a consequence of Proposition 4.3 that as our RB bubble approximations converge then the system level RBE approximation also converges:

Corollary 4.4. *If* $\sigma_1(\mu) \to 0$, $\sigma_2(\mu) \to 0$, *then* $\Delta\mathbb{U}(\mu) \to 0$.

Proof. The result directly follows from Proposition 3.1 and Lemma 4.1. □

Note we do not yet have bounds for the effectivity of our system level error estimator $\Delta\mathbb{U}(\mu)$.

In this paper we shall primarily invoke the error bound of Proposition 4.3 in particular since the different contributions to the error bound (73) are readily identified. However, it is possible to develop a sharper bound as demonstrated in

Corollary 4.5. *If* $\tilde{\lambda}_{\min}(\mu) > \sigma_1(\mu)$,

$$\|\mathbb{U}(\mu) - \widetilde{\mathbb{U}}(\mu)\|_2 \le \overline{\Delta\mathbb{U}}(\mu) \ , \tag{77}$$

where

$$\overline{\Delta\mathbb{U}}(\mu) \equiv \frac{\sigma_1(\mu) + \sigma_3(\mu) + \|\widetilde{\mathbb{F}}(\mu) - \widetilde{\mathbb{A}}(\mu)\widetilde{\mathbb{U}}(\mu)\|_2}{\tilde{\lambda}_{\min}(\mu) - \sigma_2(\mu)} \ , \tag{78}$$

and

$$\begin{aligned}
\sigma_3(\mu) \ \equiv \ &\left\{ 2 \sum_{\mathrm{COM}\in\mathcal{C}_{\mathrm{SYS}}} \left(\sum_{\text{L-P}\in\mathcal{P}_{\mathrm{COM}}} \sum_{k=1}^{n_{\mathcal{G}(\text{L-P},\mathrm{COM})}} \left(\Delta_{k,\text{L-P},\mathrm{COM}}(\mu)\right)^2 \right) \right. \\
&\left. \left(\sum_{\text{L-P}\in\mathcal{P}_{\mathrm{COM}}} \sum_{k=1}^{n_{\mathcal{G}(\text{L-P},\mathrm{COM})}} \Delta_{k,\text{L-P},\mathrm{COM}}(\mu)\ \left|\widetilde{U}^{\mathrm{COM}}_{k,\text{L-P}}(\mu)\right| \right)^2 \right\}^{1/2} . \qquad (79)
\end{aligned}$$

Note for a given $\mathrm{COM} \in \mathcal{C}_{\mathrm{SYS}}$, $\widetilde{\mathbb{U}}^{\mathrm{COM}} \in \mathbb{R}^{m_{\mathrm{COM}}}$ *is the subvector of* $\widetilde{\mathbb{U}} \in \mathbb{R}^{n_{\mathrm{sc}}}$ *with entries* $\widetilde{U}^{\mathrm{COM}}_{k,\text{L-P}} = \widetilde{U}_{k,\mathcal{G}(\text{L-P},\mathrm{COM})}$, $1 \le k \le n_{\mathcal{G}(\text{L-P},\mathrm{COM})}$, $\forall\, \text{L-P} \in \mathcal{P}_{\mathrm{COM}}$.

Proof. We first develop a (sharper) bound for

$$\left| \frac{\delta\mathbb{U}(\mu)^{\mathrm{T}}\, \delta\mathbb{A}(\mu)\, \widetilde{\mathbb{U}}(\mu)}{\delta\mathbb{U}(\mu)^{\mathrm{T}}\, \delta\mathbb{U}(\mu)} \right| . \tag{80}$$

To begin we invoke (70) to develop a bound for a single entry of the COM contribution, $(\mathbb{A}^{\mathrm{COM}} - \widetilde{\mathbb{A}}^{\mathrm{COM}})\widetilde{\mathbb{U}}^{\mathrm{COM}}$, to the vector $\delta\mathbb{A}(\mu)\, \widetilde{\mathbb{U}}(\mu)$

$$\left| \sum_{\text{L-P}\in\mathcal{P}_{\mathrm{COM}}} \sum_{k=1}^{n_{\mathcal{G}(\text{L-P},\mathrm{COM})}} \left(\mathbb{A}^{\mathrm{COM}}_{(k',\text{L-P}'),(k,\text{L-P})}(\mu) - \widetilde{\mathbb{A}}^{\mathrm{COM}}_{(k',\text{L-P}'),(k,\text{L-P})}(\mu)\right) \widetilde{U}^{\mathrm{COM}}_{(k,\text{L-P})}(\mu) \right| \le$$

$$\Delta_{k',\text{L-P}',\mathrm{COM}}(\mu) \sum_{\text{L-P}\in\mathcal{P}_{\mathrm{COM}}} \sum_{k=1}^{n_{\mathcal{G}(\text{L-P},\mathrm{COM})}} \Delta_{k,\text{L-P},\mathrm{COM}}(\mu) \left|\widetilde{U}_{k,\text{L-P},\mathrm{COM}}(\mu)\right|. \tag{81}$$

It thus follows from (81) and the Cauchy-Schwarz inequality that

$$\begin{aligned}
&\left\|(\mathbb{A}^{\mathrm{COM}}(\mu) - \widetilde{\mathbb{A}}^{\mathrm{COM}}(\mu))\widetilde{\mathbb{U}}^{\mathrm{COM}}(\mu)\right\|_2^2 \\
&\quad = \left(\sum_{\text{L-P}'\in\mathcal{P}_{\mathrm{COM}}} \sum_{k'=1}^{n_{\mathcal{G}(\text{L-P}',\mathrm{COM})}} \left(\Delta_{(k',\text{L-P}',\mathrm{COM})}(\mu) \sum_{\text{L-P}\in\mathcal{P}_{\mathrm{COM}}} \sum_{k=1}^{n_{\mathcal{G}(\text{L-P},\mathrm{COM})}} \Delta_{k,\text{L-P},\mathrm{COM}}(\mu) \left|\widetilde{U}^{\mathrm{COM}}_{k,\text{L-P}}(\mu)\right| \right)^2 \right) \\
&\quad \le \left(\sum_{\text{L-P}\in\mathcal{P}_{\mathrm{COM}}} \sum_{k=1}^{n_{\mathcal{G}(\text{L-P},\mathrm{COM})}} \Delta_{k,\text{L-P},\mathrm{COM}}(\mu)^2 \right) \left(\sum_{\text{L-P}\in\mathcal{P}_{\mathrm{COM}}} \sum_{k=1}^{n_{\mathcal{G}(\text{L-P},\mathrm{COM})}} \Delta_{k,\text{L-P},\mathrm{COM}}(\mu) \left|\widetilde{U}^{\mathrm{COM}}_{k,\text{L-P}}(\mu)\right| \right)^2 .
\end{aligned} \tag{82}$$

We now recall the assumption that a component has at most one neighbor per port; hence, with the inequality $(a+b)^2 \le 2(a^2+b^2)$, we can accumulate (82) over all $\mathrm{COM} \in \mathcal{C}_{\mathrm{SYS}}$ to obtain

$$\|\delta\mathbb{A}(\mu)\, \widetilde{\mathbb{U}}(\mu)\|_2 \le \sigma_3(\mu) . \tag{83}$$

The result then follows from (75) and (83). □

We anticipate that $\widetilde{U}_{k,\text{G-P}}$ will decrease (potentially quite rapidly) with k, and thus we can expect $\overline{\Delta\mathbb{U}}(\mu) \ll \Delta\mathbb{U}$: $\overline{\Delta\mathbb{U}}$ will be much sharper than $\Delta\mathbb{U}$. As $\overline{\Delta\mathbb{U}}(\mu)$ and $\Delta\mathbb{U}(\mu)$ can be calculated at roughly the same cost, clearly $\overline{\Delta\mathbb{U}}$ is preferred in actual computational practice.

We close this section with error analysis for the system output. An *a posteriori* error bound for the system output $s_{\mathrm{SYS}}(\mu)$ is given in

Proposition 4.6. *Suppose* $\ell_{\mathrm{SYS}} \colon X^{\mathcal{N}}_{\mathrm{SYS}} \times \mathcal{D}_{\mathrm{SYS}} \to \mathbb{R}$ *satisfies*

$$\ell_{\mathrm{SYS}}(v;\mu) = 0, \quad \forall\, v \in \bigoplus_{\mathrm{COM}\in\mathcal{C}_{\mathrm{SYS}}} X^{\mathcal{N}}_{\mathrm{COM};0} . \tag{84}$$

Then

$$|s^{\mathcal{N}}_{\mathrm{SYS}}(\mu) - \tilde{s}_{\mathrm{SYS}}(\mu)| \le \Delta\mathbb{U}^s(\mu), \tag{85}$$

for

$$\Delta\mathbb{U}^s(\mu) \equiv \Delta\mathbb{U}(\mu)\|\mathbb{L}^1(\mu)\|_2 \tag{86}$$

(and similarly, $|s^{\mathcal{N}}_{\mathrm{SYS}}(\mu) - \tilde{s}_{\mathrm{SYS}}(\mu)| \le \overline{\Delta\mathbb{U}}(\mu)\, \|\mathbb{L}^1(\mu)\|_2$*).*

Proof. From (14), (40), (42), (84), and the Cauchy-Schwarz inequality, we have

$$\begin{aligned}
\left|s^{\mathcal{N}}_{\mathrm{SYS}}(\mu) - \tilde{s}_{\mathrm{SYS}}(\mu)\right| &= \left|\ell_{\mathrm{SYS}}(u^{\mathcal{N}}_{\mathrm{SYS}}(\mu) - \tilde{u}_{\mathrm{SYS}}(\mu);\mu)\right| \\
&= \left|\sum_{\text{G-P}\in\mathcal{P}_{\mathrm{SYS}}}\sum_{k=1}^{n_{\text{G-P}}}\left(U_{k,\text{G-P}}(\mu) - \widetilde{U}_{k,\text{G-P}}(\mu)\right)\ell_{\mathrm{SYS}}(\Psi_{k,\text{G-P}};\mu)\right| \\
&\leq \left(\sum_{\text{G-P}\in\mathcal{P}_{\mathrm{SYS}}}\sum_{k=1}^{n_{\text{G-P}}}\left(U_{k,\mathcal{G}(\text{L-P,COM})}(\mu) - \widetilde{U}_{k,\mathcal{G}(\text{L-P,COM})}(\mu)\right)^2\right)^{1/2} \\
&\quad \left(\sum_{\text{G-P}\in\mathcal{P}_{\mathrm{SYS}}}\sum_{k=1}^{n_{\text{G-P}}}\ell_{\mathrm{SYS}}(\Psi_{k,\text{G-P}};\mu)^2\right)^{1/2} \\
&\leq \Delta\mathbb{U}(\mu)\left(\sum_{\text{G-P}\in\mathcal{P}_{\mathrm{SYS}}}\sum_{k=1}^{n_{\text{G-P}}}\ell_{\mathrm{SYS}}(\Psi_{k,\text{G-P}};\mu)^2\right)^{1/2}.
\end{aligned}$$

The result then follows from the definition of $\mathbb{L}^1(\mu)$ in (30). □

We note that outputs that satisfy (84) are common in applications and in particular many outputs are further defined only over ports on $\partial\Omega_{\mathrm{SYS}}$. In fact, arguably the most common outputs of interest are defined by average quantities over ports, in which case all but a few terms in the sum $\sum_{\text{G-P}\in\mathcal{P}_{\mathrm{SYS}}}\sum_{k=1}^{n_{\text{G-P}}}\ell_{\mathrm{SYS}}(\Psi_{k,\text{G-P}};\mu)^2$ in (85) will vanish. It is straightforward (but somewhat cumbersome) to extend Proposition 4.6 to the general case in which ℓ_{SYS} does not vanish over the bubble spaces and hence (84) is not satisfied. We omit this extension here since all of the outputs we consider in Section 6 do indeed satisfy (84).

A system level error bound is derived for the classical RBE method of Maday and Rønquist in [22]. A key difference between the result in [22] and Proposition 4.3 is that in our static condensation formulation we do not require component level truth calculations to estimate interface correction terms since our approximation is globally conforming.

5. Computational Considerations

We now discuss computational issues that are relevant to efficient implementation of the static condensation RBE method.

5.1. The Construction-Evaluation Decomposition

The key to the computational efficiency of the static condensation RBE method is the Construction-Evaluation (C-E) decomposition of the "standard" RB method [26]. We shall develop the C-E decomposition for reference components $\widehat{\text{COM}}$ in a Library. Ultimately, each component COM of an assembly $\mathcal{C}_{\mathrm{SYS}}$ shall be an instance of a reference component, $\widehat{\text{COM}}$, from our Library; we describe this further in the next section.

A reference component $\widehat{\text{COM}}$ is defined by a spatial domain $\Omega_{\widehat{\text{COM}}}$, a parameter domain $\mathcal{D}_{\widehat{\text{COM}}}$, parametrized bilinear and linear forms $\mu \in \mathcal{D}_{\widehat{\text{COM}}} \to a_{\widehat{\text{COM}}}(\cdot,\cdot;\mu), f_{\widehat{\text{COM}}}(\cdot;\mu)$, and a collection of ports $\mathcal{P}_{\widehat{\text{COM}}}$ and port domains $\Gamma_{\widehat{\text{L-P}}}, \forall\, \widehat{\text{L-P}} \in \mathcal{P}_{\widehat{\text{COM}}}$. We presume that $a_{\widehat{\text{COM}}}$ is symmetric, continuous over $H^1(\Omega_{\widehat{\text{COM}}})$, and coercive over $\{v \in H^1(\Omega_{\widehat{\text{COM}}})\colon v|_{\Gamma_{\widehat{\text{L-P}}}} = 0, \forall\, \widehat{\text{L-P}} \in \mathcal{P}_{\widehat{\text{COM}}}\}$; we further assume that f is continuous over $H^1(\Omega_{\widehat{\text{COM}}})$. The truth discretization of the reference component $\widehat{\text{COM}}$ can be decomposed into port and bubble degrees of freedom. We denote by $n_{\widehat{\text{L-P}},\widehat{\text{COM}}}$ the number of interface functions $\psi_{k,\widehat{\text{L-P}},\widehat{\text{COM}}}$ on $\widehat{\text{L-P}}, \widehat{\text{COM}}$; we further define $m_{\widehat{\text{COM}}} \equiv \sum_{\widehat{\text{L-P}}\in\mathcal{P}_{\widehat{\text{COM}}}} n_{\widehat{\text{L-P}},\widehat{\text{COM}}}$, and thus $m_{\widehat{\text{COM}}}$ represents the total number of port degrees of freedom in $\widehat{\text{COM}}$. Also, we let $m_{\max} \equiv \max_{\widehat{\text{COM}}\in\text{Library}} m_{\widehat{\text{COM}}}$.

For any given $\widehat{\text{COM}}$ in the Library, $\tilde{b}_{f,\widehat{\text{COM}}} \in \widetilde{X}_{f,\widehat{\text{COM}};0}$ and $\tilde{b}_{k,\widehat{\text{L-P}},\widehat{\text{COM}}} \in \tilde{X}_{k,\widehat{\text{L-P}},\widehat{\text{COM}};0}$, $1 \le k \le n_{\widehat{\text{L-P}},\widehat{\text{COM}}}$, $\forall\, \widehat{\text{L-P}} \in \mathcal{P}_{\widehat{\text{COM}}}$, satisfy hatted (38) and hatted (39), respectively. (Here the adjective "hatted" shall refer to a $\widehat{\text{COM}}$ version of an equation earlier defined for a particular instance COM; we thus avoid much repetition.) The contribution of these RB bubble functions to the approximate Schur complement and load vector, $\mu \in \mathcal{D}_{\widehat{\text{COM}}} \rightarrow \mathbb{A}^{\widehat{\text{COM}}}(\mu), \mathbb{F}^{\widehat{\text{COM}}}(\mu)$, are then given by hatted (49) and hatted (50), respectively. The corresponding *a posteriori* error bound for $\left|\mathbb{A}^{\widehat{\text{COM}}}_{(k',\widehat{\text{L-P}}'),(k,\widehat{\text{L-P}})}(\mu) - \widetilde{\mathbb{A}}^{\widehat{\text{COM}}}_{(k',\widehat{\text{L-P}}),(k,\widehat{\text{L-P}})}(\mu)\right|$ is given from (70) by $\Delta_{k,\widehat{\text{L-P}},\widehat{\text{COM}}}(\mu)\, \Delta_{k',\widehat{\text{L-P}}',\widehat{\text{COM}}}(\mu)$ for $\Delta_{k,\widehat{\text{L-P}},\widehat{\text{COM}}}(\mu)$ defined in hatted (65). Similarly, the *a posteriori* error bound for $\left|\mathbb{F}^{\widehat{\text{COM}}}_{k',\widehat{\text{L-P}}'}(\mu) - \widetilde{\mathbb{F}}^{\widehat{\text{COM}}}_{k',\widehat{\text{L-P}}}(\mu)\right|$ is given by $\Delta_{f,\widehat{\text{COM}}}(\mu)\, \Delta_{k',\widehat{\text{L-P}}',\widehat{\text{COM}}}(\mu)$.

The C-E decomposition effects the computation of $\widetilde{\mathbb{A}}^{\widehat{\text{COM}}}(\mu), \widetilde{\mathbb{F}}^{\widehat{\text{COM}}}(\mu)$, and $\Delta_{f,\widehat{\text{COM}}}(\mu)$, $\Delta_{k,\widehat{\text{L-P}},\widehat{\text{COM}}}(\mu)$, $1 \le k \le n_{\widehat{\text{L-P}},\widehat{\text{COM}}}, \forall\, \widehat{\text{L-P}} \in \mathcal{P}_{\widehat{\text{COM}}}$, in two steps: The first, Construction, step is performed only once; this step is expensive and in particular the cost shall depend on $\dim(X^{\mathcal{N}}_{\widehat{\text{COM}};0})$, the $\widehat{\text{COM}}$ truth bubble space. The second, Evaluation, step is performed many times for each new parameter of interest in $\mathcal{D}_{\widehat{\text{COM}}}$; this step is inexpensive and in particular the cost shall be *independent* of $\dim(X^{\mathcal{N}}_{\widehat{\text{COM}};0})$. We now describe the C-E steps in more detail: for brevity, we focus on $\widetilde{\mathbb{A}}^{\widehat{\text{COM}}}$ and the associated error bounds $\Delta_{k,\widehat{\text{L-P}},\widehat{\text{COM}}}(\mu)$, $1 \le k \le n_{\widehat{\text{L-P}},\widehat{\text{COM}}}, \forall\, \widehat{\text{L-P}} \in \mathcal{P}_{\widehat{\text{COM}}}$.

We must first introduce an additional critical enabling hypothesis on the bilinear and linear forms. In particular, we suppose that for each $\widehat{\text{COM}} \in$ Library, $a_{\widehat{\text{COM}}}$ and $f_{\widehat{\text{COM}}}$ are "affine in functions of the parameter": for any $\mu \in \mathcal{D}_{\widehat{\text{COM}}}$,

$$a_{\widehat{\text{COM}}}(v,w;\mu) \;\equiv\; \sum_{q=1}^{Q_{a,\widehat{\text{COM}}}} \Theta^q_{a,\widehat{\text{COM}}}(\mu)\, a^q_{\widehat{\text{COM}}}(v,w), \tag{87}$$

$$f_{\widehat{\text{COM}}}(v;\mu) \;\equiv\; \sum_{q=1}^{Q_{f,\widehat{\text{COM}}}} \Theta^q_{f,\widehat{\text{COM}}}(\mu)\, f^q_{\widehat{\text{COM}}}(v), \tag{88}$$

where $\Theta^q_{a,\widehat{\text{COM}}}, \Theta^q_{f,\widehat{\text{COM}}} \colon \mathcal{D}_{\widehat{\text{COM}}} \rightarrow \mathbb{R}$ are *parameter dependent* functions and $a^q_{\widehat{\text{COM}}} \colon X^{\mathcal{N}}_{\text{SYS}} \times X^{\mathcal{N}}_{\text{SYS}} \rightarrow \mathbb{R}$, $f^q_{\widehat{\text{COM}}} \colon X^{\mathcal{N}}_{\text{SYS}} \rightarrow \mathbb{R}$ are *parameter independent* forms. This hypothesis can be relaxed via the Empirical Interpolation Method (EIM) [3], which enables us to recover an *approximate* affine decomposition. However, very often (87),(88) is exactly satisfied, and for the numerical examples of the next section this is indeed the case.

We first discuss the Construction step. We consider a given $\widehat{\text{COM}} \in$ Library, a given $\widehat{\text{L-P}} \in \mathcal{P}_{\widehat{\text{COM}}}$, and for that port, a given mode $k \in \{1, \ldots, n_{\widehat{\text{L-P}},\widehat{\text{COM}}}\}$. We then apply a Greedy procedure to form $\widetilde{X}^N_{k,\widehat{\text{L-P}},\widehat{\text{COM}}}$, $1 \le N \le N_{\max,[k,\widehat{\text{L-P}},\widehat{\text{COM}}]}$; we note that

$$\widetilde{X}^1_{k,\widehat{\text{L-P}},\widehat{\text{COM}}} \subset \widetilde{X}^2_{k,\widehat{\text{L-P}},\widehat{\text{COM}}} \subset \cdots \subset \widetilde{X}^{N_{\max,[k,\widehat{\text{L-P}},\widehat{\text{COM}}]}}_{k,\widehat{\text{L-P}},\widehat{\text{COM}}}$$

constitutes a set of *hierarchical* RB approximation spaces. We may then choose, for each $[k, \widehat{\text{L-P}}, \widehat{\text{COM}}]$,

$$\widetilde{X}_{k,\widehat{\text{L-P}},\widehat{\text{COM}};0} = \widetilde{X}^{N_{[k,\widehat{\text{L-P}},\widehat{\text{COM}}]}}_{k,\widehat{\text{L-P}},\widehat{\text{COM}}},$$

for $N_{[k,\widehat{\text{L-P}},\widehat{\text{COM}}]} \in \{1, \ldots, N_{\max,[k,\widehat{\text{L-P}},\widehat{\text{COM}}]}\}$ selected according to various error or cost criteria. We must also compute and store (for the Evaluation stage) various inner products over $X^{\mathcal{N}}_{\widehat{\text{COM}};0}$, the collection of which we shall denote the Evaluation Dataset.

We now present operation counts for the *Evaluation* stage, which shall be the emphasis of our discussion. For simplicity we present our operation counts in terms of

$$N \equiv \max_{\widehat{\text{COM}} \in \text{Library},\, \widehat{\text{L-P}} \in \mathcal{P}_{\widehat{\text{COM}}},\, k \in \{1,\ldots,n_{\widehat{\text{L-P}},\widehat{\text{COM}})}\}} N_{\max,[k,\widehat{\text{L-P}},\widehat{\text{COM}}]}$$

and

$$Q = \max_{\widehat{\text{COM}} \in \text{Library}} [Q_{a,\widehat{\text{COM}}}, Q_{f,\widehat{\text{COM}}}] \ .$$

In actual practice $N_{[k,\widehat{\text{L-P}},\widehat{\text{COM}}]}$ may be selected (in the Evaluation step) considerably less than N for many $[k,\widehat{\text{L-P}},\widehat{\text{COM}}]$, and hence our estimates are perforce pessimistic. Also, some $\widehat{\text{COM}} \in$ Library may not be invoked in any particular system.

We first consider the computation of the RB bubbles. We consider a particular $[k,\widehat{\text{L-P}},\widehat{\text{COM}}]$: Given any $\mu \in \mathcal{D}_{\widehat{\text{COM}}}$, we will require $O(QN^2) + O(N^3)$ FLOPs to obtain $\tilde{b}_{k,\widehat{\text{L-P}},\widehat{\text{COM}}}(\mu)$ (or, more precisely, to obtain the *coefficients* of the reduced basis expansion for $\tilde{b}_{k,\widehat{\text{L-P}},\widehat{\text{COM}}}$); we will then additionally require $O(Q^2N^2)$ FLOPs to obtain $\Delta_{k,\widehat{\text{L-P}},\widehat{\text{COM}}}(\mu)$, our *a posteriori* bound for the error in $\tilde{b}_{k,\widehat{\text{L-P}},\widehat{\text{COM}}}(\mu)$ relative to $b^{\mathcal{N}}_{k,\widehat{\text{L-P}},\widehat{\text{COM}}}(\mu)$. The Evaluation storage is $O(Q^2N^2)$. If we now sum over all port degrees of freedom in $\widehat{\text{COM}}$ we require $O(m_{\widehat{\text{COM}}}(Q^2N^2 + N^3))$ FLOPs ; in addition, we contribute $O(m_{\widehat{\text{COM}}}Q^2N^2)$ storage to the Evaluation Dataset.

We next consider the operation count to evaluate the RB contributions to $\widetilde{\mathbb{A}}$ in terms of the *now known* RB bubble functions (basis coefficients). We first consider a particular $k, \widehat{\text{L-P}}, \widehat{\text{COM}}$ and $k', \widehat{\text{L-P}}', \widehat{\text{COM}}$: Given any $\mu \in \mathcal{D}_{\widehat{\text{COM}}}$, $\widetilde{\mathbb{A}}^{\widehat{\text{COM}}}_{(k,\widehat{\text{L-P}}),(k',\widehat{\text{L-P}}')}(\mu)$ of (49) may be evaluated in $O(QN^2)$ operations. Note we may think of $\widetilde{\mathbb{A}}^{\widehat{\text{COM}}}_{(k,\widehat{\text{L-P}}),(k',\widehat{\text{L-P}}')}(\mu)$ as a joint "Schur entry" output associated with $\tilde{b}_{k,\widehat{\text{L-P}},\widehat{\text{COM}}}$ and $\tilde{b}_{k',\widehat{\text{L-P}}',\widehat{\text{COM}}}$. If we now sum over all port degrees of freedom in $\widehat{\text{COM}}$ we require $O(m^2_{\widehat{\text{COM}}}QN^2)$ FLOPs; we also contribute $O(m^2_{\widehat{\text{COM}}}QN^2)$ storage to the Evaluation Dataset.

5.2. **Offline-Online Decomposition**

The static condensation RBE method proceeds in two stages. In the Offline stage, for each $\widehat{\text{COM}} \in$ Library, we perform the Construction step to obtain the Evaluation Dataset. In the Online stage, we assemble a system of components COM $\in \mathcal{C}_{\text{SYS}}$ as instances of $\widehat{\text{COM}} \in$ Library, and we then invoke Evaluation to compute $\mu \in \mathcal{D}_{\text{SYS}} \rightarrow \tilde{s}_{\text{SYS}}(\mu), \Delta\mathbb{U}^s(\mu)$. Note that the Offline stage involves both Construction and (in the Greeedy procedure) Evaluation, however the Online stage involves only Evaluation.

5.2.1. *Offline Stage*

For each $\widehat{\text{COM}} \in$ Library, we perform the following steps:

Offline 1. For each $\widehat{\text{L-P}} \in \mathcal{P}_{\widehat{\text{COM}}}$ — each distinct port in $\widehat{\text{COM}}$ — we compute the port eigenmodes from hatted (8).

Offline 2. For each $k \in \{1,\ldots,n_{\widehat{\text{L-P}},\widehat{\text{COM}}}\}$, $\forall\, \widehat{\text{L-P}} \in \mathcal{P}_{\widehat{\text{COM}}}$, we compute the elliptically lifted interface functions from hatted (11), (12), and (13).

Offline 3. For each $k \in \{1,\ldots,n_{\widehat{\text{L-P}},\widehat{\text{COM}}}\}$, $\forall\, \widehat{\text{L-P}} \in \mathcal{P}_{\widehat{\text{COM}}}$, we perform the Greedy algorithm [25] to form the RB spaces $\widetilde{X}^{\bullet}_{k,\widehat{\text{L-P}},\widehat{\text{COM}}}$.

Offline 4. If $f_{\widehat{\text{COM}}} \neq 0$: We perform the Greedy algorithm to form the "source" RB bubble space $\widetilde{X}_{f,\widehat{\text{COM}}}$.

Offline 5. We form and store the necessary inner products in the Evaluation Dataset.

The computational burden of this construction procedure can be significant. We note that the $m_{\widehat{\text{COM}}}$ (or $m_{\widehat{\text{COM}}} + 1$ if $f_{\widehat{\text{COM}}} \neq 0$) invocations of the Greedy algorithm are completely independent and can therefore be straightforwardly parallelized [20].

5.2.2. *Online Stage*

The Online stage comprises two substages: the assembly of the system; the parametric analysis of the system. To assemble the system we first define a collection of components $\mathcal{C}_{\rm SYS}$ in which each COM $\in \mathcal{C}_{\rm SYS}$ is an instantiation of a $\widehat{\rm COM} \in$ Library; we shall denote by $|\mathcal{C}_{\rm SYS}|$ the number of components in the system. Note that many COM may be instantiated from a single reference component $\widehat{\rm COM}$. We next define the local-port to global-port mapping $\mathcal{G}$ which provides all necessary component connectivity information and indeed $\mathcal{P}^0_{\rm SYS}$ is the image of $\mathcal{G}$; we may then impose Dirichlet boundary conditions on selected ports to identify $\mathcal{P}_{\rm SYS}$ (which we assume yields a well-posed problem over $\Omega_{\rm SYS}$). Finally, we provide the system parameter domain $\mathcal{D}_{\rm SYS} \subset \prod_{{\rm COM}\in\mathcal{C}_{\rm SYS}} \mathcal{D}_{\rm COM}$. This process is closely related to assembly of a finite element system from a set of reference elements except of course that our $\Omega_{\rm COM}$ remain reference elements from a geometric perspective and a final affine map is required to realize the physical domain.

Geometry requires some special consideration. In particular, we recall that $\widehat{\rm COM}$ and hence COM is defined over a domain $\Omega_{\rm COM}$ which is independent of μ; μ-dependent geometric variations are implicit through transformations reflected in the coefficients of $a_{\rm COM}$, $f_{\rm COM}$. The actual physical domain associated with a component COM is given by $\Omega^{\rm phys}_{\rm COM}(\mu) \equiv \mathcal{A}_{\rm COM}(\Omega_{\rm COM};\mu)$ for $\mu \in \mathcal{D}_{\rm COM}$, where $\mathcal{A}_{\rm COM}(\,\cdot\,;\mu)$ is a piecewise-affine mapping; the system physical domain is thus given by

$$\overline{\Omega}^{\rm phys}_{\rm SYS}(\mu) \equiv \bigcup_{{\rm COM}\in\mathcal{C}_{\rm SYS}} \overline{\mathcal{A}}_{\rm COM}(\Omega_{\rm COM};\mu)\ .$$

In the simplest case $\mathcal{A}_{\rm COM}(\cdot;\mu)$ may be dictated solely by translation and rotation "docking" parameters; for isotropic, homogeneous operators, our forms $a_{\rm COM}$ and $f_{\rm COM}$ will be *independent* of these docking parameters. On the other hand, $a_{\rm COM}$, $f_{\rm COM}$ will of course depend on geometric parameters μ that represent dilations and other more general affine transformations.

It is clear that we do not have complete freedom in imposing component connections: two crucial connectivity constraints must be honored. We consider two components ${\rm COM}, {\rm COM}'$ which are connected in the sense that $\exists\, {\rm L\text{-}P} \in \mathcal{P}_{\rm COM}$ and ${\rm L\text{-}P}' \in \mathcal{P}_{{\rm COM}'}$ such that $\mathcal{G}({\rm L\text{-}P}, {\rm COM}) = \mathcal{G}({\rm L\text{-}P}', {\rm COM}')$. First, for such connected components, the associated truth "trace" spaces over the shared port must be identical: $X^{\mathcal{N}}(\Gamma_{\rm L\text{-}P,COM}) = X^{\mathcal{N}}(\Gamma_{\rm L\text{-}P',COM'})$. This constraint imposes a condition on the set of possible connections and hence possible mappings $\mathcal{G}$. Second, for connected components, $\mathcal{A}_{\rm COM}(\Gamma_{\rm L\text{-}P,COM};\mu \in \mathcal{D}_{\rm COM})$ must coincide with $\mathcal{A}_{\rm COM'}(\Gamma_{\rm L\text{-}P',COM'};\mu \in \mathcal{D}_{\rm COM'})$. This constraint imposes a condition on $\mathcal{D}_{\rm SYS}$, in particular on the allowable domains for those parameters related to geometry (and hence on which $\mathcal{A}_{\rm COM}$ will depend).

We now consider the steps and associated operation counts and storage required to evaluate $\mu \in \mathcal{D}_{\rm SYS} \rightarrow \tilde{s}_{\rm SYS}(\mu), \Delta\mathbb{U}^s(\mu)$. Typically we expect that a system defined by $\mathcal{C}_{\rm SYS}, \mathcal{P}_{\rm SYS}$ will be analyzed for many $\mu \in \mathcal{D}_{\rm SYS}$, though of course only a single evaluation is also permitted: the advantage of the RBE approach — amortization of the Offline stage by many appeals to the Online stage — can be realized either over many parameters for a particular system or over many systems (or both).

Given $\mu \in \mathcal{D}_{\rm SYS}$ ($\Rightarrow \mu \in \mathcal{D}_{\rm COM}$, COM $\in \mathcal{C}_{\rm SYS}$), we perform the following steps:

Online 1. We Evaluate the set of $m_{\rm COM}$ (or $m_{\rm COM}+1$, if $f_{\rm COM} \neq 0$) RB bubble approximations (coefficients) and associated error bounds for each COM $\in \mathcal{C}_{\rm SYS}$: the total cost over all components is $O(|\mathcal{C}_{\rm SYS}|\, m_{\rm max}(N^3 + Q^2N^2 + QN^2))$ FLOPs and the total storage is $O(|\mathcal{C}_{\rm SYS}|\, m_{\rm max}(Q^2N^2 + QN^2))$. The complexity scales with $|\mathcal{C}_{\rm SYS}|$ even if |Library| $\ll |\mathcal{C}_{\rm SYS}|$ since $\mu \in \mathcal{D}_{\rm COM}$ is potentially different for different instances COM of any particular reference component $\widehat{\rm COM}$.

Online 2. We Evaluate the "local stiffness matrices" and "local load vectors" for each COM $\in \mathcal{C}_{\rm SYS}$ and then assemble $\widetilde{\mathbb{A}}$ of (44) according to Algorithm 2 at total cost $O(|\mathcal{C}_{\rm SYS}| m^2_{\rm max} QN^2)$. The complexity again scales with $|\mathcal{C}_{\rm SYS}|$ because different instances of a reference component $\widehat{\rm COM}$ may potentially correspond to different parameter values; the complexity scales with $m^2_{\rm max}$ since $\widetilde{\mathbb{A}}^{\rm COM}$ has entries for each *pair* $({\rm L\text{-}P}, {\rm COM}), ({\rm L\text{-}P}', {\rm COM}')$.

Online 3. We accumulate the error bound terms for $\sigma_1(\mu)$ and $\sigma_2(\mu)$ of Proposition 4.3 (and $\sigma_3(\mu)$ of Corollary 4.5) at total cost $O(|\mathcal{C}_{\rm SYS}|\, m_{\rm max})$.

Online 4. We solve the linear system (44) for $\widetilde{\mathbb{U}}(\mu)$ and then compute $\tilde{s}_{\rm SYS}(\mu)$ from (45) at total cost $O(n_{\rm sc}\, m^2_{\rm max})$.

Online 5. We compute $\tilde{\lambda}_{\min}(\mu)$ and evaluate the system field and output *a posteriori* error bounds $\Delta\mathbb{U}$ of (72) and $\Delta\mathbb{U}^s$ of (85) at total cost $O(n_{\rm sc}\, m_{\max}^2)$.

We typically solve for $\widetilde{\mathbb{U}}(\mu)$ by LU factorization (though for larger statically condensed systems it will be preferable to employ iterative methods [6] in particular given the moderate condition number of $\tilde{\mathbb{A}}$ [7]), and evaluate $\tilde{\lambda}_{\min}(\mu)$ by inverse iteration (or, for large systems, the Lanczos algorithm). The computational costs in Online 4 and Online 5 assume that $\widetilde{\mathbb{A}}(\mu)$ is a block sparse matrix with bandwidth $m_{\max}$; we further assume that evaluation of $\tilde{\lambda}_{\min}(\mu)$ requires $O(1)$ iterations.

In actual practice we also visualize the field. Typically we would visualize $\tilde{u}_{\rm SYS}(\mu)$ over selected regions or surfaces of $\Omega_{\rm SYS}$, S. If these selected regions coincide with ports then no additional effort is required. If, however, these selected regions include parts of $\partial\Omega_{\rm SYS}$ (or $\Omega_{\rm SYS}$) which do not coincide with ports, then additional operations and storage are required — $O(N|V|)$, where V is the set of points in Ω at which $\tilde{u}_{\rm SYS}$ must be evaluated in order to render the solution over S.

The static condensation RBE method addresses one of the major disadvantages of the standard RB method: treatment of "many parameter" systems. Previous work has demonstrated the viability of the standard RB method for problems with up to ~ 25 parameters [20,27], but these many-parameter problems require a large number of RB basis functions (large N) and consequently significant computational effort in the Offline stage and also the Online stage — recall that the Online complexity scales cubically with N. In contrast, the static condensation RBE approach can treat $O(100)$ parameters with relative ease since we implicitly "factorize" the parameter domain: in the Offline stage we define a Library of components each of which possesses only a few parameters — hence low-dimensional RB spaces will typically suffice for each component; then, in the Online stage, we can straightforwardly connect many components together in order to efficiently model many-parameter systems. Put differently, the static condensation RBE method permits us to create a wide range of different systems — including topological variations — in the Online stage; this gain in Online flexibility relative to the standard RB, a transfer of jurisdiction from the Offline stage to the Online stage, implicitly increases the number of parameters which can be accommodated. The price we pay for this, however, is that the RBE approach will typically contain more degrees of freedom than a standard RB approximation: *many* ($m_{\rm COM}$ for component COM) simultaneous RB models, each of size N; potentially many port degrees of freedom — large $m_{\rm COM}$ and/or $n_{\rm sc}$. We first discuss the "N," and then the $m_{\rm COM}$ (which determines, from $|\mathcal{C}_{\rm SYS}|$, $n_{\rm sc}$).

First, we note that the port lifting function $\Psi_{k,\text{G-P}}$ will decay rapidly into the components (see Figure 2) and we thus anticipate that for larger k the corresponding bubbles will be less sensitive to parameters — hence for these modes we can anticipate increasingly small RB spaces. The latter is particularly important for computational performance as we refine our truth discretization.

Second, we note that often a component will include as a parameter a uniform (over $\widehat{\rm COM}$) material property. Such parameters, potentially different in each instance COM of a reference element $\widehat{\rm COM}$, will then scale out of the component bubble equations; these parameters do not affect the dimension of the RB spaces on COM and are therefore handled "for free" by the static condensation RBE approach. More precisely, these parameters are treated exclusively by the interface functions at no additional computational cost. (This feature is of course shared by the truth formulation of Section 2.2, but it has no effect on computational efficiency in that case since a fixed "truth" bubble space is employed on each component.)

Third, we note that although in the examples of this paper we consider a standard Greedy approach, in practice the Online RB costs can also be greatly reduced by application of *h-p* (in parameter) approaches [11]. In the *h-p* approach we would develop optimal decompositions of $\mathcal{D}_{\widehat{\rm COM}}$ and then develop a lower order RB on each parameter subdomain of $\mathcal{D}_{\rm COM}$. For any given parameter in $\mathcal{D}_{\widehat{\rm COM}}$ we thus invoke a smaller RB model (associated with the relevant parameter *sub*domain): we therefore effect a reduction in N.

Fourth, practical engineering systems often contain many repeated components (an original motivation for the classical RBEM [22, 23]). In the static condensation RBE approach, replication corresponds to a system that contains several identical physical components — components that share both a parent reference component $\widehat{\rm COM}$ and a particular parameter value in $\mathcal{D}_{\widehat{\rm COM}}$: the "local stiffness matrix" and "local load vector" for all of these components will be the same, and hence we can obtain significant economies in the assembly stage by appropriate "caching" of data. Similarly, engineering analysis and design often follows an incremental path. In the static condensation RBE approach a path corresponds to small modifications to

a system which is already assembled — a change to a few parameters, a small modification to component connectivity, or the addition/removal of a few components: the local stiffness matrix and local load vector for most of the system remains unchanged, and hence we can again realize computational savings. In particular, in both these perturbative situations, Online 1 through Online 3 can be skipped for all repeated/unchanged components — in effect, in these not-so-special circumstances, we *eliminate* most of the RB-related costs associated with system analysis.

We now turn to $m_{\widehat{\text{COM}}}$, which determines (with $|\mathcal{C}_{\text{SYS}}|$) n_{sc}. We assume that in general $|\mathcal{C}_{\text{SYS}}|$ will be relatively large — at least $O(10)$ — to exercise the advantage of the RBE approach. We thus focus on $m_{\widehat{\text{COM}}}$. First, it is clear that if we consider "quasi-one-dimensional" systems — components with significant internal complexity but simple port structure [4] — then we may arguably choose $m_{\widehat{\text{COM}}}$ small in our truth discretization.[3] We can be more rigorous: in each reference component we prescribe $m_{\widehat{\text{COM}}}$ large as always (which implies associated $n_{\text{G-P}}$ large) — in order to err on the good side of the truth; we then retain (Online) for any system port G-P $\in \mathcal{P}_{\text{SYS}}$ only the $n'_{\text{G-P}} < n_{\text{G-P}}$ basis functions $\widetilde{\Phi}_{k,\text{G-P}}(\mu)$, $1 \le k \le n'_{\text{G-P}}$, associated with the lowest modes — in effect, a "port-reduced" space $\widetilde{X}'_{\mathcal{P}_{\text{SYS}}} \subset \widetilde{X}_{\mathcal{P}_{\text{SYS}}}$; we construct a port-reduced stiffness matrix and load vector, $\widetilde{\mathbb{A}}'$ and $\widetilde{\mathbb{F}}'$, respectively, in terms of the retained modes — the higher modes are removed; we obtain a port-reduced $\widetilde{\mathbb{U}}'$ from (44) with $\widetilde{\mathbb{A}}$ and $\widetilde{\mathbb{F}}$ replaced by $\widetilde{\mathbb{A}}'$ and $\widetilde{\mathbb{F}}'$, respectively; we find a port-reduced $\tilde{\lambda}'_{\text{min}}$ from the definition (37) with $\widetilde{\mathbb{A}}$ replaced by $\widetilde{\mathbb{A}}'$; we bound the error due to port reduction in $\widetilde{\mathbb{U}}'$ by our error bound (73) (note the residual term will now be *non-zero*), and the error due to port reduction in $\tilde{\lambda}'_{\text{min}}$ by the eigenproblem residual norm [15, 18]. We thus save significantly in Online 2 since even for the error bounds (residual evaluation) we need only compute the columns of $\widetilde{\mathbb{A}}$ associated with the retained modes. And of course we save in Online 4 and Online 5 due to the reduction in dimension of the linear system and eigenproblem, respectively. There is one chink in the rigor: the eigenproblem residual norm is a bound for the error in $\tilde{\lambda}'_{\text{min}}$ only if $\tilde{\lambda}'_{\text{min}}$ is closer to $\tilde{\lambda}_{\text{min}} = \tilde{\lambda}_1$ than to $\tilde{\lambda}_2$; this is plausible — since we retain the low modes associated with the port expansions — but not certain.

6. Numerical Results

In this section we present numerical results to demonstrate the capabilities of the static condensation RBE method. We present results for model problems from heat transfer and solid mechanics. The results presented here are obtained with `rbOOmit` [20], `libMesh` [19], and Matlab.

6.1. Heat Transfer Example

We begin with the heat transfer example in which we model a scalar temperature field in a three dimensional domain; this problem satisfies all hypotheses of the analysis presented in the preceding sections. It is simplest to build up our system level description of the problem from the component level. We consider three reference components in our Library: (*i*) a "stem" component, (*ii*) a "plate" component, and (*iii*) a "T"-junction connector. These components are shown schematically in Figure 3.

Let $\widehat{\text{COM}}_1$ denote the stem reference component associated with the domain $\Omega_{\widehat{\text{COM}}_1} \equiv (0, 0.4) \times (0, 0.4) \times (0, 3)$. The domain $\Omega_{\widehat{\text{COM}}_1}$ is meshed with $4 \times 4 \times 30$ Q_1 ($d = 3$) elements. As shown in Figure 3, $\widehat{\text{COM}}_1$ has two ports, $\Gamma_{\widehat{\text{L-P}}_1,\widehat{\text{COM}}_1} \equiv (0, 0.4) \times (0, 0.4) \times \{0\}$ and $\Gamma_{\widehat{\text{L-P}}_2,\widehat{\text{COM}}_1} \equiv (0, 0.4) \times (0, 0.4) \times \{3\}$. We consider three (non-dimensional) parameters: $\mu_1 \in [0.001, 0.01]$ denotes the Biot number on the entire component boundary $\partial\Omega_{\widehat{\text{COM}}_1}$, $\mu_2 \in [2/3, 4/3]$ denotes the vertical scaling of the stem (relative to the "default" height of 3), and $\mu_3 \in [0.5, 2]$ denotes the uniform thermal conductivity of the stem relative to a reference conductivity; hence $\mathcal{D}_{\widehat{\text{COM}}_1} \equiv [0.001, 0.01] \times [2/3, 4/3] \times [0.5, 2]$. We consider equilibrium conduction over $\Omega^{\text{phys}}_{\widehat{\text{COM}}_1} \equiv \mathcal{A}_{\widehat{\text{COM}}_1}(\Omega_{\widehat{\text{COM}}_1}; \mu_2) = (0.4) \times (0.4) \times (0, 3\mu_2)$ (we also permit translation and rotation) for a medium of conductivity μ_3 exposed to a Robin (heat transfer) coefficient μ_1 and subject to uniform unity (in our nondimensionalization) volumetric heat generation.

[3] Note however that eigenfunction expansions (and modal synthesis approaches [28]) in general will not achieve overly rapid convergence rates as is well established in the context of spectral methods [14]. We exploit here the simpler argument that for quasi-one-dimensional components there should be relatively little transverse variation in the solution.

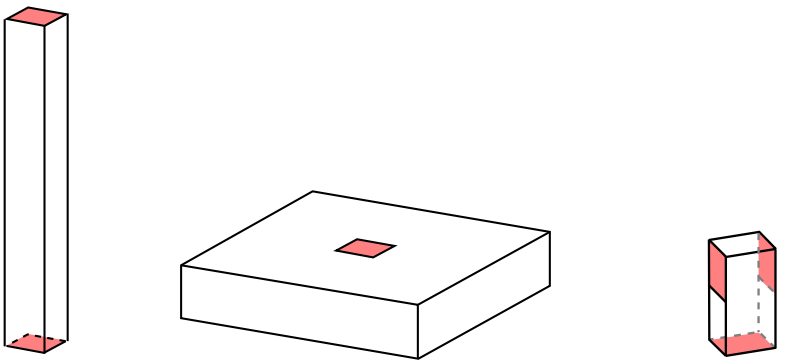

stem component plate component "T"-junction component

FIGURE 3. Three reference components for the heat transfer Library: $\widehat{\text{COM}}_1 \equiv$ stem, $\widehat{\text{COM}}_2 \equiv$ plate, $\widehat{\text{COM}}_3 \equiv$ T. Ports are shaded in red.

Then we have

$$a_{\widehat{\text{COM}}_1}(v,w;\mu) \equiv \sum_{q=1}^{5} \Theta^q_{a,\widehat{\text{COM}}_1}(\mu) a^q_{\widehat{\text{COM}}_1}(v,w), \tag{89}$$

where

$$\Theta^1_{a,\widehat{\text{COM}}_1}(\mu) \equiv \mu_2\mu_3,\ \Theta^2_{a,\widehat{\text{COM}}_1}(\mu) \equiv \mu_3/\mu_2,\ \Theta^3_{a,\widehat{\text{COM}}_1}(\mu) \equiv \mu_1\mu_2\mu_3,$$
$$\Theta^4_{a,\widehat{\text{COM}}_1}(\mu) \equiv P_1\mu_1\mu_3, \Theta^5_{a,\widehat{\text{COM}}_1}(\mu) \equiv P_2\mu_1\mu_3, \tag{90}$$

and

$$a^1_{\widehat{\text{COM}}_1}(v,w) \equiv \int_{\Omega_{\widehat{\text{COM}}_1}} (v_x w_x + v_y w_y), \tag{91}$$

$$a^2_{\widehat{\text{COM}}_1}(v,w) \equiv \int_{\Omega_{\widehat{\text{COM}}_1}} v_z w_z, \tag{92}$$

$$a^3_{\widehat{\text{COM}}_1}(v,w) \equiv \int_{\partial\Omega_{\widehat{\text{COM}}_1} \setminus \left(\Gamma_{\widehat{\text{L-P}}_1,\widehat{\text{COM}}_1} \cup \Gamma_{\widehat{\text{L-P}}_2,\widehat{\text{COM}}_1}\right)} vw, \tag{93}$$

$$a^4_{\widehat{\text{COM}}_1}(v,w) \equiv \int_{\Gamma_{\widehat{\text{L-P}}_1,\widehat{\text{COM}}_1}} vw, \tag{94}$$

$$a^5_{\widehat{\text{COM}}_1}(v,w) \equiv \int_{\Gamma^2_{\widehat{\text{L-P}}_2,\widehat{\text{COM}}_1}} vw; \tag{95}$$

also, we define a volumetric source term on $\widehat{\text{COM}}_1$,

$$f_{\widehat{\text{COM}}_1}(v;\mu) \equiv \mu_2 \int_{\Omega_{\widehat{\text{COM}}_1}} v. \tag{96}$$

Both $a_{\widehat{\text{COM}}_1}$ and $f_{\widehat{\text{COM}}_1}$ satisfy the "affine" hypothesis (87), (88), which enables efficient reduced basis approximation through the C-E decomposition.

We employ for the $\widehat{\text{COM}}_1$ inner product

$$(v,w)_{X,\widehat{\text{COM}}_1} \equiv \int_{\Omega_{\widehat{\text{COM}}_1}} (v_x w_x + v_y w_y)\mu_{3,\min}\mu_{2,\min} + (v_z w_z)\mu_{3,\min}/\mu_{2,\max}, \tag{97}$$

where $\mu_{2,\min} = 2/3$, and $\mu_{3,\min} = 0.5$, $\mu_{2,\max} = 4/3$. With this choice we may set $\alpha^{\rm LB}_{\widehat{\rm COM}_1} \equiv 1$ for the coercivity constant lower bound; note the coercivity constant is defined relative to the *bubble spaces* $X^{\mathcal{N}}_{\widehat{\rm COM}_1;0}$ and hence the semi-norm suffices. Note that $\|\cdot\|_{X,\rm COM} = \|\cdot\|_{X,\widehat{\rm COM}}$ for each instance COM of $\widehat{\rm COM}$; then $\|v\|_{X,\rm SYS} = \sum_{\rm COM\in\mathcal{C}_{SYS}} \|v|_{\Omega_{\rm COM}}\|_{X,\rm COM}$.

We observe that the operators $a^4_{\widehat{\rm COM}_1}$ and $a^5_{\widehat{\rm COM}_1}$ vanish for all $v, w \in X^{\mathcal{N}}_{\widehat{\rm COM}_1;0}$; these terms are included in the formulation to permit us to impose general natural boundary conditions on the ports via the interface functions. To wit, we include scalars $P_1, P_2 \in \{0,1\}$ in order to turn the port Biot terms "on" or "off" as desired. For example, we would set $P_1 = 0$ if a stem component has a connection on port $\Gamma_{\widehat{\text{L-P}}_1,\widehat{\rm COM}_1}$; similarly, we would set $P_1 = 0$ if there is no connection on $\Gamma_{\widehat{\text{L-P}}_1,\widehat{\rm COM}_1}$ but we wish to impose a homogeneous Neumann condition on $\Gamma_{\widehat{\text{L-P}}_1,\widehat{\rm COM}_1}$. On the other hand, we would set $P_1 = 1$ if we wish to impose a Robin condition on $\Gamma_{\widehat{\text{L-P}}_1,\widehat{\rm COM}_1}$. In essence, we take advantage of the general port treatment to impose general boundary conditions.

The other two components of the heat transfer Library represent similar physics but in different geometries; we shall define the geometric domains and parameters for these components, but omit the component operator equations for the sake of brevity. Let $\widehat{\rm COM}_2$ denote the plate reference component, with the domain $\Omega_{\widehat{\rm COM}_2} \equiv (0,2.4)\times(0,2.4)\times(0,0.5)$. The plate reference geometry is meshed with $24\times24\times5$ Q_1 ($d=3$) elements. The plate $\widehat{\rm COM}_2$ has two ports at $\Gamma_{\widehat{\text{L-P}}_1,\widehat{\rm COM}_2} \equiv (1,1.4)\times(1,1.4)\times\{0\}$ and $\Gamma_{\widehat{\text{L-P}}_2,\widehat{\rm COM}_2} \equiv (1,1.4)\times(1,1.4)\times\{0.5\}$, and four (non-dimensional) parameters: $\mu_1 \in [0.001, 0.01]$ denotes the Biot number on $\Gamma_{\widehat{\rm COM}_2}$, $\mu_2 \in [2/3, 4/3]$ denotes the vertical scaling of the plate (relative to the "default" height of 0.5), $\mu_3 \in [0.5, 2]$ denotes the thermal conductivity of $\widehat{\rm COM}_2$ relative to a reference conductivity, and $\mu_4 \in [0.5, 2]$ denotes the horizontal scaling of the plate in the "non-port region" $\Omega_{\widehat{\rm COM}_2} \setminus (1,1.4)\times(1,1.4)\times(0,0.5)$ such that for $\mu_4 = 0.5$ (respectively, $\mu_4 = 2.0$) the plate is of horizontal extent 1.4×1.4 (respectively, 4.4×4.4). Also, we set $f_{\widehat{\rm COM}_2} \equiv 0$. Similarly, let $\widehat{\rm COM}_3$ be the "T"-junction connector reference component. In this case $\Omega_{\widehat{\rm COM}_3} \equiv (0,0.4)\times(0,0.4)\times(0,0.8)$. The geometry is meshed with $4\times4\times8$ Q_1 ($d=3$) elements. The "T" $\widehat{\rm COM}_3$ has three ports: $\Gamma_{\widehat{\text{L-P}}_1,\widehat{\rm COM}_3} \equiv (0,0.4)\times(0,0.4)\times\{0\}$, $\Gamma_{\widehat{\text{L-P}}_2,\widehat{\rm COM}_3} \equiv (0,0.4)\times\{0\}\times(0.4,0.8)$, and $\Gamma_{\widehat{\text{L-P}}_3,\widehat{\rm COM}_3} \equiv (0,0.4)\times\{0.4\}\times(0.4,0.8)$. This component has only two parameters: $\mu_1 \in [0.001, 0.01]$ denotes the Biot number on $\Gamma_{\widehat{\rm COM}_3}$, and $\mu_2 \in [0.5, 2]$ denotes the thermal conductivity of $\widehat{\rm COM}_3$ relative to a reference conductivity. We set $f_{\widehat{\rm COM}_3}$ to be a uniform volumetric source term analogous to $f_{\widehat{\rm COM}_1}$.

We note that for $\widehat{\rm COM}_1$, $\widehat{\rm COM}_2$, and $\widehat{\rm COM}_3$, the thermal conductivity parameter scales out of (39). This can be seen (in the case of $\widehat{\rm COM}_1$) from the presence of the μ_3 factor in each $\Theta^q_{a,\widehat{\rm COM}_1}$ in (90): thus $a_{\rm COM}$ scales linearly with μ_3, and hence from (39) the bubble is independent of μ_3. (Note to achieve this independence we scale the Biot number by the conductivity and not the reference conductivity.) Therefore, as discussed earlier, the thermal conductivity is a "free" parameter with regards to the reduced basis approximation for the bubble functions of (39). In fact, it is not only free as regards the cost of the RB approximation, but also free in the sense that μ_3 can take on any positive value quite independent of the definition of $\mathcal{D}_{\widehat{\rm COM}_1}$.

We recall one subtlety as regards geometric configuration. In fact, all three components actually include additional parameters related to arbitrary translation and rotation: these parameters docking determine the map $\mathcal{A}_{\rm COM}(\cdot,\mu)$ which serves to position COM; we omit these additional "free" parameters from our formal definition of $\mathcal{D}_{\widehat{\rm COM}}$ since for our *isotropic homogeneous* components the bilinear forms are invariant with respect to translation and rotation. More generally — but not in our examples — it will be of interest to include uniform dilation parameters which would permit variable "sizing" within the system; in our examples here, such a uniform dilation parameter would not be free due to Robin terms.

We now generate the three reference components introduced above. We have 25 nodes on each port, hence $m_{\widehat{\rm COM}_1} = m_{\widehat{\rm COM}_2} = 50$, and $m_{\widehat{\rm COM}_3} = 75$. For each component, we set the (absolute) tolerance for termination of the Greedy algorithm to 10^{-5}, and we also set the limit for the dimension of the RB spaces (for each $k, \widehat{\text{L-P}}$) to $N_{\max,\lim} = 15$. We present in Figure 4 a plot of $N_{\max,[k,\widehat{\text{L-P}}_1,\widehat{\rm COM}_1]}$ for $1 \le k \le 25$. We do observe that in general the dimensions of the RB spaces are relatively low and furthermore that

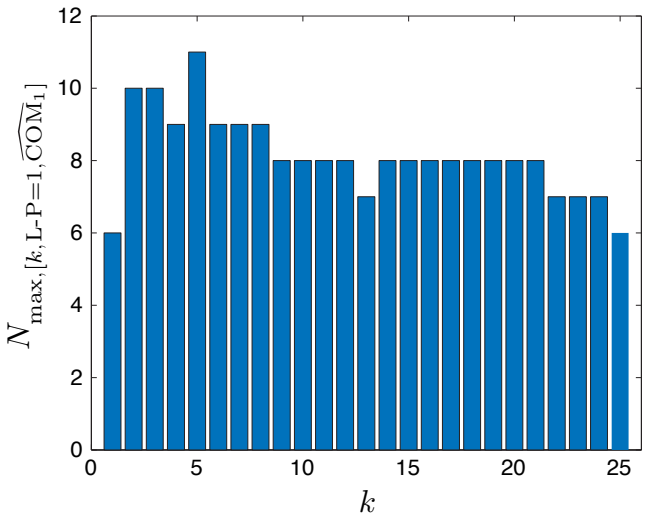

FIGURE 4. The dimension of the RB spaces on port $\widehat{\text{L-P}}_1$ of $\widehat{\text{COM}}_1$, $N_{\max,[k,\widehat{\text{L-P}}_1,\widehat{\text{COM}}_1]}$ for modes $1 \le k \le 25$.

the dimensions of the RB spaces appear to decrease slowly with k — as suggested by the rapid decay of the $\psi_{k,\text{L-P,COM}} + \tilde{b}_{k,\text{L-P,COM}}(\mu)$ into the interior of COM. Note that the component $\widehat{\text{COM}}_2$ has one more parameter and more complicated geometric variations; as a result, in this case all RB spaces saturate at the $N_{\max,\text{lim}} = 15$ limit.

We now consider the Online stage. In all cases we set $N_{[k,\text{L-P,COM}]} = N_{\max,[k,\widehat{\text{L-P}},\widehat{\text{COM}}]}$ for L-P, COM an instantiation of $\widehat{\text{L-P}}, \widehat{\text{COM}}$. To demonstrate the flexibility of the static condensation RBE method we shall assemble and solve several different systems from the three references components introduced above. We first consider a system with 6 stem components and 5 plates — 6 instantiations of $\widehat{\text{COM}}_1$ and 5 instantiations of $\widehat{\text{COM}}_2$. We "stack" the components vertically in the order (starting at the base) $\text{stem}_1 \to \text{plate}_1 \to \text{stem}_2 \to \text{plate}_2 \to \ldots \to \text{stem}_6$. We also introduce two system outputs: $s_{\text{SYS},1}(\mu)$ is the average temperature over the base port of stem_1, and $s_{\text{SYS},2}(\mu)$ is the average temperature on the top port of stem_3. This system has 38 parameters in total; note for this system $\mathcal{D}_{\text{SYS}}$ is simply the tensor product of the $\mathcal{D}_{\text{COM}}$.

For our first analysis, the stem parameters are

$$\begin{aligned} &\mu_{\text{stem}_1} \equiv (0.01, 0.67, 1.2), \quad \mu_{\text{stem}_2} \equiv (0.0075, 1, 1), \quad \mu_{\text{stem}_3} \equiv (0.002, 1.33, 0.5), \\ &\mu_{\text{stem}_4} \equiv (0.002, 1.33, 0.5), \quad \mu_{\text{stem}_5} \equiv (0.0075, 1, 1), \quad \mu_{\text{stem}_6} \equiv (0.01, 0.67, 1.2); \end{aligned} \tag{98}$$

the plate parameters are

$$\begin{aligned} \mu_{\text{plate}_1} \equiv (0.01, 1.33, 1, 0.75), \quad \mu_{\text{plate}_2} \equiv (0.01, 1, 1, 1), \quad \mu_{\text{plate}_3} \equiv (0.005, 0.67, 1, 0.5), \\ \mu_{\text{plate}_4} \equiv (0.01, 1, 1, 1), \quad \mu_{\text{plate}_5} \equiv (0.01, 1.33, 1, 0.75). \end{aligned} \tag{99}$$

We set P_1 and P_2 in order to impose a heat transfer (Robin) boundary condition on the bottom port of stem_1 and the top port of stem_6.

The system temperature profile is shown in Figure 5(A); the associated RB system outputs are $\tilde{s}_{\text{SYS},1}(\mu) = 4.10$, $\tilde{s}_{\text{SYS},2}(\mu) = 7.85$. We obtain the field output bound $\Delta\mathbb{U}(\mu) = 0.24$, and the system output error bound $\Delta\mathbb{U}^s(\mu) = 0.62$ for both $\tilde{s}_{\text{SYS},1}(\mu)$ and $\tilde{s}_{\text{SYS},2}(\mu)$. The true field error is $\|\mathbb{U}(\mu) - \widetilde{\mathbb{U}}(\mu)\|_2 = 4.62 \times 10^{-5}$; the truth solution is computed via the truth static condensation approach of Section 2.3 (and requires computation time of 191 seconds[4]). The effectivity of the error bound $\Delta\mathbb{U}(\mu)/\|\mathbb{U}(\mu) - \widetilde{\mathbb{U}}(\mu)\|_2 = 5.37 \times 10^3$ is quite

[4]In this case it would be more computationally efficient to solve for $\mathbb{U}(\mu)$ via the classical finite element method. However, the static condensation approach is more convenient here since it eliminates the need to directly mesh Ω_{SYS}. Note for the

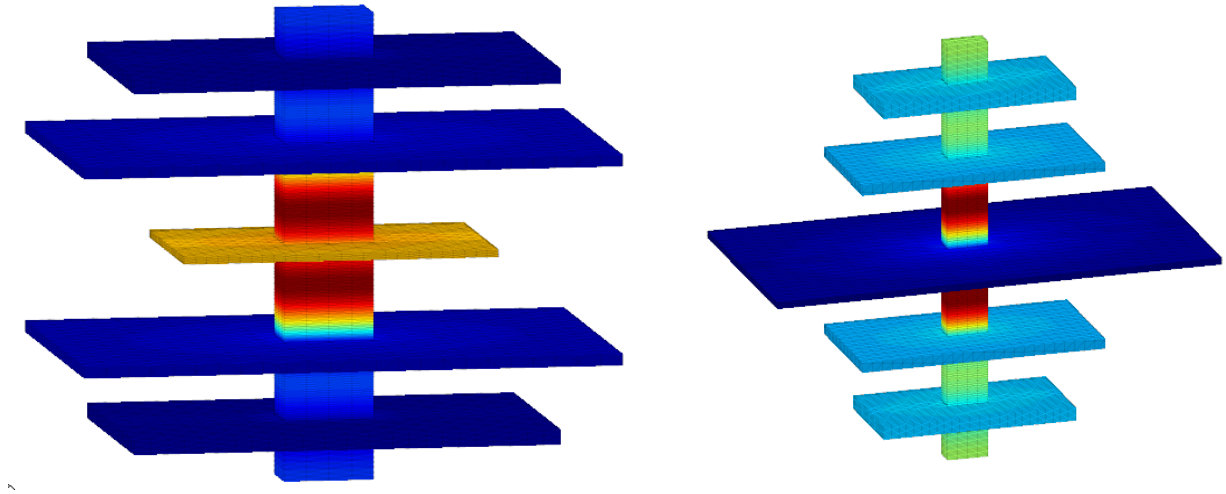

(A) Solution $\tilde{u}_{\mathrm{SYS}}(\mu)$ over $\Omega^{\mathrm{phys}}_{\mathrm{SYS}}(\mu)$ for parameters defined in (98), (99); minimum is 3.0 (blue), maximum is 9.7 (red).

(B) Solution $\tilde{u}_{\mathrm{SYS}}(\mu)$ over $\Omega^{\mathrm{phys}}_{\mathrm{SYS}}(\mu)$ for the parameters defined in (98), (99), except that $\mu_4 = 2$ for plate 3; minimum is 1.36 (blue), maximum is 6.42 (red).

FIGURE 5. Temperature profiles for our system with 6 stems and 5 plates for two different values of the parameters.

poor; however, when we employ the sharper error bound $\overline{\Delta\mathbb{U}}(\mu)$ we obtain an effectivity $\overline{\Delta\mathbb{U}}(\mu)/\|\mathbb{U}(\mu) - \widetilde{\mathbb{U}}(\mu)\|_2 = 3.24 \times 10^2$, which is certainly improved and commensurate with standard RB error bound effectivities reported in the literature.

The static condensation system is of dimension $n_{\mathrm{sc}} = 300$ — compared to $\dim(X^{\mathcal{N}}_{\mathrm{SYS}}) = 38{,}900$; we enjoy here the benefits of the "quasi-one-dimensional" limit with relatively few port degrees of freedom compared to interior degrees of freedom. The Online computation time in this case is 0.72 seconds, of which 0.67 seconds are devoted to the RB steps Online 1 – Online 3 and the remainder to solution of the Schur complement system (Online 4) and calculation of the Schur complement minimum eigenvalue (Online 5). All computation times reported in Section 6.1 are based on an AMD Opteron 2382 processor.

We next demonstrate a "parameter sweep": we predict the field and outputs of our system as we vary the "horizontal scaling" parameter μ_4 for plate$_3$, say H, from 0.5 to 2; we hold all other parameters fixed per (98),(99). Figure 5(A) presents the temperature field for $H = 0.5$, while Figure 5(B) presents the temperature profile for $H = 2$; Figure 6(A) and Figure 6(B) provide a detail of plate$_3$ extracted from Figure 5(A) and 5(B), respectively. We note that the change in H results in a significant change in the overall temperature as well as the temperature distribution. We show in Figure 7 the system output $\tilde{s}_{\mathrm{SYS},2}(\mu)$ and associated output error bounds at 21 parameters in the range $[0.5, 2]$; the error bounds confirm at least 10% accuracy. As indicated in Section 5.2.2, we can skip assembly calculations for any unchanged components; as a result, for each parameter value H, steps Online 1 – Online 3 now require only 0.10 seconds (rather than 0.67 if we assemble "from scratch") and total analysis time is 0.15 seconds (rather than 0.72).

We now consider a system which has many repeated components. We instantiate 15 stems and 14 plates and stack them in the same way (stem → plate → stem) as in our first system. In this case we set zero Neumann boundary conditions on the bottom and top ports of stem$_1$ and stem$_{15}$, respectively. This system accommodates up to 101 independent parameters, however for our homogeneous system we set each stem parameter to $\mu_{\mathrm{stem}} \equiv (0.01, 1, 1)$, and each plate parameter to $\mu_{\mathrm{plate}} \equiv (0.008, 1, 1, 1)$. The solution field is shown in Figure 8(A); we obtain a relative error bound of $\Delta\mathbb{U}(\mu)/\|\widetilde{\mathbb{U}}(\mu)\|_2 = 0.011$. The dimension of the static condensation system is $n_{\mathrm{sc}} = 750$ — compared to $\dim(X^{\mathcal{N}}_{\mathrm{SYS}}) = 107{,}500$. As a result of component

static condensation RBE method, and earlier RBE approaches, we need never form the mesh for Ω_{SYS} and indeed need never compute the truth $u^{\mathcal{N}}_{\mathrm{SYS}}$.

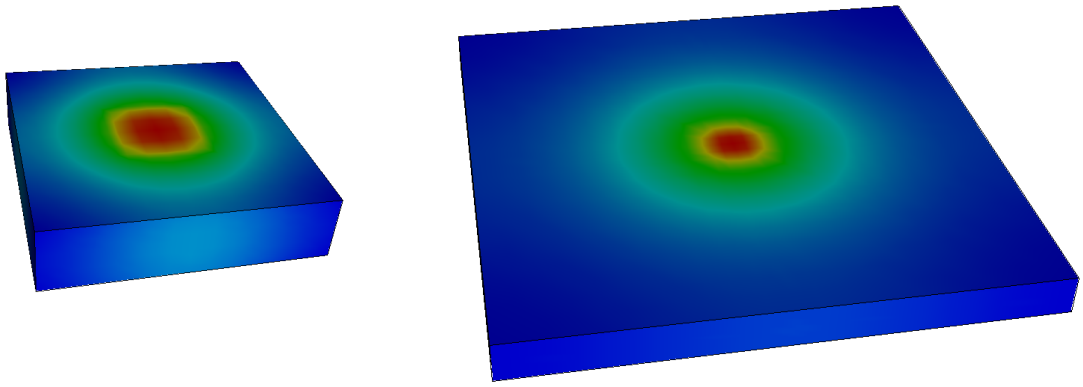

]

(A) Detail of plate_3 from Figure 5(A); minimum is 7.52 (blue), maximum is 7.90 (red).

(B) Detail of plate_3 from Figure 5(B); minimum is 1.36 (blue), maximum is 2.20 (red).

FIGURE 6. Temperature profiles for our system with 6 stems and 5 plates: detail for the middle plate.

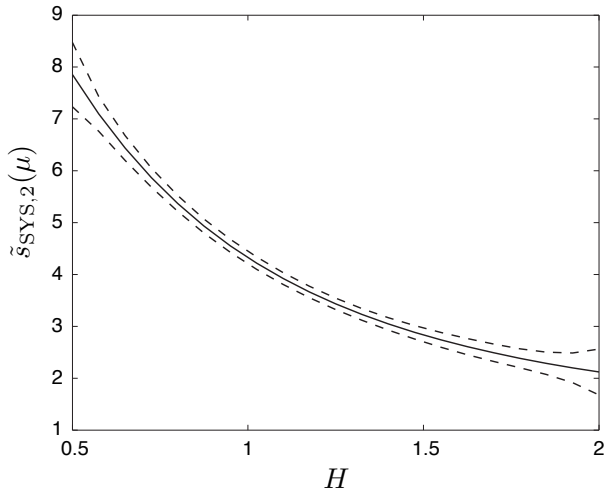

FIGURE 7. Plot of $\tilde{s}_{\text{SYS},2}(\mu)$ (solid line) and error bounds (dashed lines) at 21 evenly spaced parameters for the plate_3 horizontal scaling parameter H in the range $[0.5, 2]$ — all other parameters are as defined in (98), (99).

repetition, we only need to assemble local stiffness matrices and load vectors for two components: the resulting Online computation time is 0.26 seconds. Note that caching of repeated local stiffness matrices and load vectors leads to a reduction in the assembly time for the Schur complement system — steps Online 1 – Online 3 — from 1.71 seconds to 0.12 seconds.

As our next example we modify our repeated-component system: we now disconnect leg_4 from plate_4 to introduce a "crack." Note we set $P_2 = 0$ on leg_4 to impose a zero Neumann condition on the crack; this yields a slightly larger static condensation system, $n_{\text{sc}} = 775$. The temperature field in this case is shown in Figure 8(B): the crack leads to a significantly higher temperature in leg_4, as expected; the accuracy of the prediction is confirmed by the relative error bound $\Delta\mathbb{U}(\mu)/\|\widetilde{\mathbb{U}}(\mu)\|_2 = 0.0108$. Assembly of this system

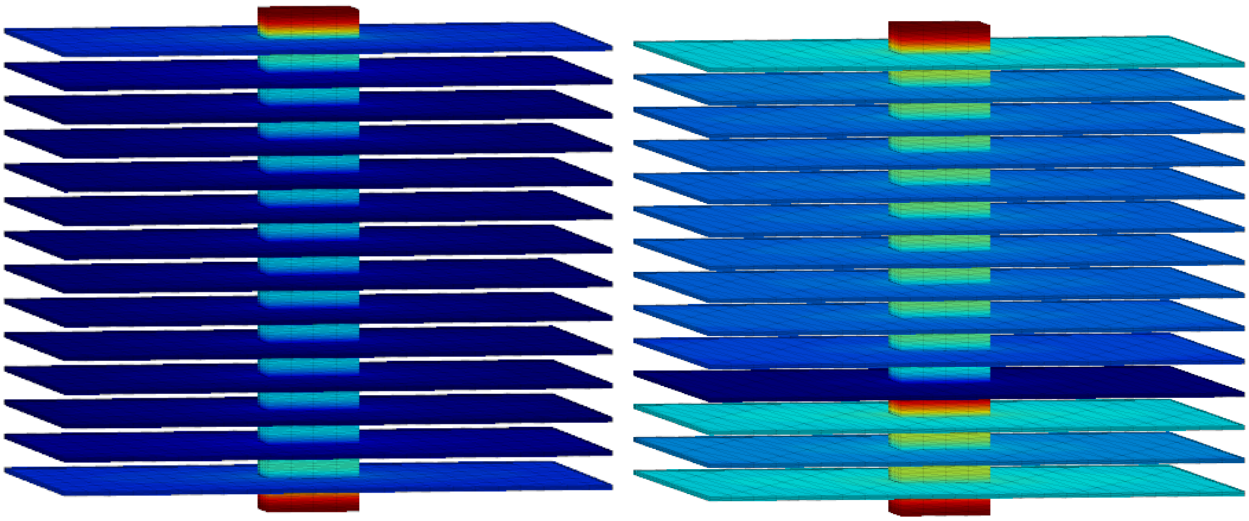

(A) "Repeated component" system; minimum is 2.50 (blue), maximum is 5.49 (red).

(B) "Repeated component" system with "crack" between leg_4 and plate_4; minimum is 1.64 (blue), maximum is 5.50 (red).

FIGURE 8. Temperature fields for two system configurations with 15 identical stems and 14 identical plates.

again requires only 0.12 seconds. This example illustrates the ease with which we may consider topology variations.

Finally, as our last thermal case we construct the system shown in Figure 9 which contains all three types of reference components: the system contains 7 stems, 3 plates, and 3 "T"-junction components. The component names are given in Figure 9, and the parameters are set as follows

$$\begin{aligned}
&\mu_{\text{stem}_1} \equiv (0.01, 1, 1), \quad \mu_{\text{stem}_2} \equiv (0.01, 1, 1.25), \quad \mu_{\text{stem}_3} \equiv (0.01, 1, 1), \quad \mu_{\text{stem}_4} \equiv (0.01, 1, 1.2),\\
&\mu_{\text{stem}_5} \equiv (0.005, 1, 1), \quad \mu_{\text{stem}_6} \equiv (0.01, 0.7, 1), \quad \mu_{\text{stem}_7} \equiv (0.01, 0.7, 1),\\
&\mu_{\text{plate}_1} \equiv (0.01, 1, 1, 1), \quad \mu_{\text{plate}_2} \equiv (0.008, 1, 1.2, 0.8), \quad \mu_{\text{plate}_3} \equiv (0.01, 1, 1, 1),\\
&\mu_{\text{T-junction}_1} \equiv (0.01, 1), \quad \mu_{\text{T-junction}_2} \equiv (0.001, 1), \quad \mu_{\text{T-junction}_3} \equiv (0.005, 1).
\end{aligned}$$

The temperature field is shown in Figure 9; the relative error bound $\Delta\mathbb{U}(\mu)/\|\widetilde{\mathbb{U}}(\mu)\|_2 = 0.014$ indicates 1% accuracy. Here $n_{\text{sc}} = 425$ compared to $\dim(X^{\mathcal{N}}_{\text{SYS}}) = 26{,}425$; the Online computation time is 0.56 seconds. This example illustrates the good side of the curse of dimensionality: we obtain combinatorial flexibility in system design but cost increases only algebraically.

6.2. **Solid Mechanics Example**

We now move to the solid mechanics example. In this case, the solution is a vector field of displacements. The port mode and interface function constructions directly apply to this case, except that we now solve vector problems in (8) and (11), (12), (13). In this case, well-posedness of the Schur complement system relies on Korn's inequality, and we do not analyze this issue here — though we do note that our *a posteriori* error bound results in Proposition 4.3 and Proposition 4.6 still apply.

We consider the two reference components shown in Figure 10: (*i*) a "pillar" component, and (*ii*) an "arch" component. Let $\widehat{\text{COM}}_1$ denote the pillar reference component with domain $\Omega_{\widehat{\text{COM}}_1} = (0,1) \times (0,5)$ as shown in Figure 10(A). The pillar $\widehat{\text{COM}}_1$ has two ports corresponding to the bottom and top boundaries of the domain, respectively. We consider three (non-dimensional) parameters: $\mu_1 \in [0.1, 10]$ denotes the height scaling of the pillar, $\mu_2 \in [1, 10]$ denotes the Young's modulus relative to a reference value, and $\mu_3 \in$

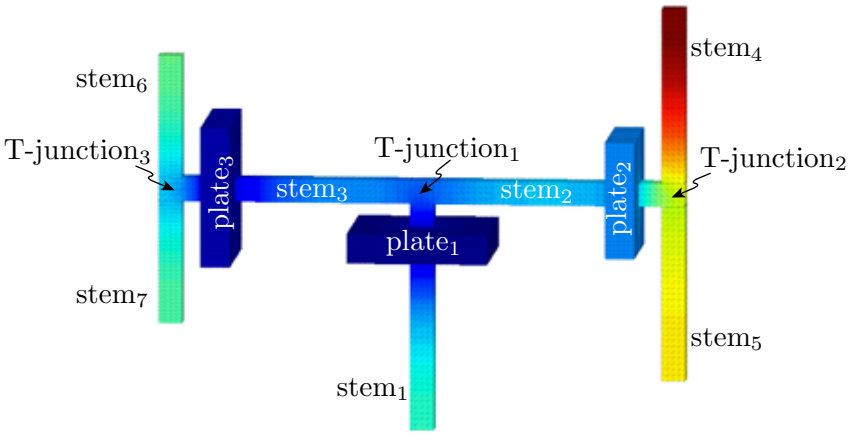

FIGURE 9. Temperature field for a system which contains all three types of thermal components; minimum is 3.24 (blue), maximum is 9.06 (red).

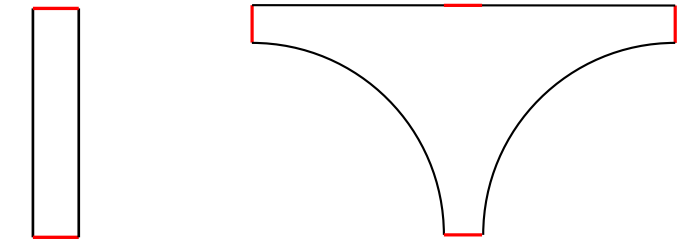

(A) pillar (B) arch

FIGURE 10. The two components of the bridge structure Library: $\widehat{\text{COM}}_1 \equiv$ pillar, $\widehat{\text{COM}}_2 \equiv$ arch. Ports are shaded in red.

$[10^{-7}, 10^{-6}]$ represents the material density. (The small magnitude of μ_3 is due to the ratio of gravitational and elastic stress effects for realistic values of the Young's modulus.) We consider equilibrium elasticity over $\mathcal{A}_{\widehat{\text{COM}}_1}(\Omega_{\widehat{\text{COM}}_1}; \mu_1) = (0,1) \times (0, \mu_1)$ (we also permit translations but not rotations) for a linear isotropic medium with Young's modulus μ_2 subject to a uniform body force μ_3 in the (negative) vertical direction; note we could also permit rotations in $\mathcal{A}$ but this docking parameter would also need to appear in f. We refer to [26] for the construction of the operators; the affine forms (87), (88) are recovered with $Q_{a,\widehat{\text{COM}}} = 3$ and $Q_{f,\widehat{\text{COM}}} = 1$.

Let $\widehat{\text{COM}}_2$ denote the arch reference component with domain $\Omega_{\widehat{\text{COM}}_2}$. The arch $\widehat{\text{COM}}_2$ has four ports corresponding to the four boundaries shown in Figure 10(B). We consider two (non-dimensional) parameters: $\mu_1 \in [1, 10]$ denotes the Young's modulus relative to a reference value, and $\mu_2 \in [10^{-7}, 10^{-6}]$ represents the material density. The physical model is again a linear isotropic medium subject to a uniform body force. The affine forms (87), (88) obtain: in this case, given the absence of geometric variations, $Q_{a,\widehat{\text{COM}}} = Q_{f,\widehat{\text{COM}}} = 1$.

For both $\widehat{\text{COM}}_1$ and $\widehat{\text{COM}}_2$ the parameters corresponding to the Young's modulus and the material density are both free. The component $\widehat{\text{COM}}_2$ is particularly simple: the Young's modulus μ_1 scales a in both (38) and (39); the material density μ_2 scales (only) the right-hand side of (38). It follows that for $\widehat{\text{COM}}_2$ there are in fact no "real" parameters: in (38) , the bubble functions scale as $1/\mu_1$; in (39) the bubble function scales as μ_2/μ_1.

We now generate the two components of our library. We have 5 nodes on each port, and since the problem is defined for a vector (displacement field), we obtain $n_{\widehat{\text{COM}}_1} = 20$ and $n_{\widehat{\text{COM}}_2} = 40$. We set the (relative)

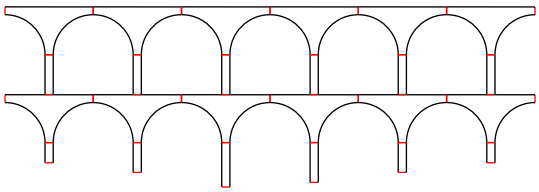

FIGURE 11. The Pont du Gard bridge structure.

tolerance for termination of the Greedy algorithm for each component to 10^{-5} or $N_{\max,\text{lim}} = 15$. For the pillar component we obtain $N_{\max,[k,\widehat{\text{L-P}},\widehat{\text{COM}}_1]} = 15$ over all nodes and ports. For the arch component we obtain $N_{\max,[k,\widehat{\text{L-P}},\widehat{\text{COM}}_2]} = 1$ over all nodes and ports (and also $N_{\max,[f,\widehat{\text{COM}}_2]} = 1$ for $\widetilde{X}_{f,\widehat{\text{COM}}_2;0}$): the RB Greedy algorithm detects the free parameters automatically.

We then consider the Online stage. In all cases we set $N_{[k,\text{L-P,COM}]} = N_{\max,[k,\widehat{\text{L-P}},\widehat{\text{COM}}]}$ for COM an instantiation of $\widehat{\text{COM}}$. We first consider a "Pont du Gard" system consisting of four layers of components stacked as shown in Figure 11. The first and the third layers have 6 pillar components each; and the second and fourth layers have 6 arch components each. The ordering of the first and second layers are $\text{pillar}_1 \rightarrow \text{pillar}_2 \rightarrow \ldots \rightarrow \text{pillar}_6$, and $\text{arch}_1 \rightarrow \text{arch}_2 \rightarrow \ldots \rightarrow \text{arch}_6$, respectively, from the left to the right; similarly, the ordering for the third and fourth layers are $\text{pillar}_7 \rightarrow \ldots \rightarrow \text{pillar}_{12}$ and $\text{arch}_7 \rightarrow \ldots \rightarrow \text{arch}_{12}$. We also introduce our system output: $s_{\text{SYS}}(\mu)$ is the vertical displacement of the top port of arch_3. The system has 60 parameters in total; note, however, that in this system $\mathcal{D}_{\text{SYS}} \neq \Pi_{\text{COM}\in\text{C}_{\text{SYS}}}\mathcal{D}_{\text{COM}}$ since all the pillars in the third layer must be of the same length μ_1.

For our first analysis we set pillar parameters for the first layer to

$$\begin{aligned} &\mu_{\text{pillar}_1} \equiv (3, 1, 10^{-7}), \quad \mu_{\text{pillar}_2} \equiv (4, 1, 10^{-7}), \quad \mu_{\text{pillar}_3} \equiv (6, 1, 10^{-7}), \\ &\mu_{\text{pillar}_4} \equiv (5, 1, 10^{-7}), \quad \mu_{\text{pillar}_5} \equiv (4, 1, 10^{-7}), \quad \mu_{\text{pillar}_6} \equiv (3, 1, 10^{-7}); \end{aligned} \tag{100}$$

all pillar parameters in the third layer are set to

$$\mu_{\text{pillar}_7} = \mu_{\text{pillar}_8} = \mu_{\text{pillar}_9} = \mu_{\text{pillar}_{10}} = \mu_{\text{pillar}_{11}} = \mu_{\text{pillar}_{12}} \equiv (6, 1, 10^{-7}); \tag{101}$$

all the arch parameters are set to $\mu_{\text{arch}} = (1, 10^{-7})$. (The situation is depicted in Figure 11.) We apply (zero) Dirichlet boundary conditions on all the bottom ports of all the pillars on the bottom (foundation) layer, as well as on the four arch ports on the extreme left and extreme right sides of the structure.

The displacement field of the structure is shown in Figure 12(A). The associated RBE system output is $\tilde{s}_{\text{SYS}}(\mu) = -5.65 \times 10^{-5}$. We obtained the field output bound $\Delta\mathbb{U}(\mu) = 1.537 \times 10^{-7}$ and the system output error bound $\Delta\mathbb{U}^s = 9.72 \times 10^{-8}$. The true field error is $\|\mathbb{U}(\mu) - \widetilde{\mathbb{U}}(\mu)\|_2 = 4.47 \times 10^{-9}$ (the truth solution is computed via the truth static condensation approach of Section 2.3 and requires computation time of 46 seconds): the effectivity of the error bound $\Delta\mathbb{U}(\mu)/\|\mathbb{U}(\mu) - \widetilde{\mathbb{U}}(\mu)\|_2 = 34.38$, which is very good; we can further improve this result to $\overline{\Delta\mathbb{U}}(\mu)/\|\mathbb{U}(\mu) - \widetilde{\mathbb{U}}(\mu)\|_2 = 17.43$. The static condensation system is of size $n_{\text{sc}} = 440$ — compared to $\dim(X^{\mathcal{N}}_{\text{SYS}}) = 23{,}208$. The Online computation time in this case is 1.62 seconds, of which 1.5 seconds are devoted to Online 1 – Online 3; due to repeated components in each layer we need perform RB calculations for only 7 different pillar components and only 1 arch component.

We next demonstrate a "parameter sweep": we predict the field and output of our system as we vary the height H of (all) the pillars in the third layer from 0.5 to 10; we hold all the other parameters fixed per (100),(101) and $\mu_{\text{arch}} = (1, 10^{-7})$. We show two displacement fields for two different values of H, $H = 6$ and $H = 1$, in Figure 12. We present in Figure 13 the output $\tilde{s}_{\text{SYS}}(\mu)$ and associated error bounds at 20 parameter values in the range [0.5,10]. As indicated in Section 5.2.2, we can skip assembly calculations for unchanged components: in this case, for each new value of the sweep parameter we only need to recalculate data for one pillar component; Online 1 – Online 3 now require only 0.21 seconds (rather than 1.5 seconds if we assemble "from scratch") and total analysis time is just 0.32 seconds (rather than 1.62 seconds).

(A) $H = 6$ (B) $H = 1$

FIGURE 12. Displacement field of the bridge for different values of the height H of (all) the pillars in the third layer; the displacement field is scaled by a factor of 40,000.

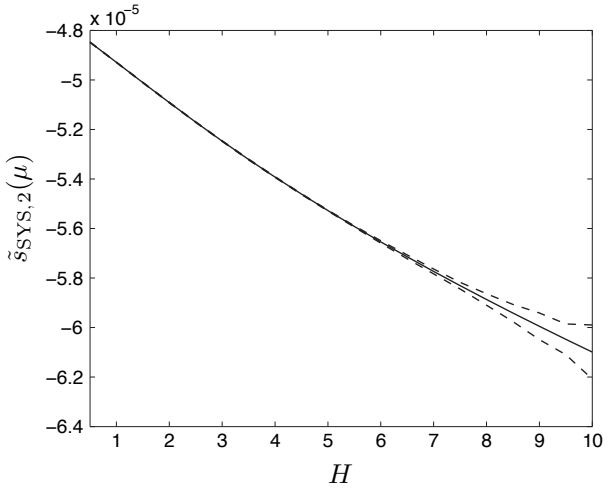

FIGURE 13. Plot of $\tilde{s}_{\mathrm{SYS}}(\mu)$ (solid line) and error bounds (dashed lines) at 20 evenly spaced values of H.

For our final example, we consider the same structure as in Figure 11, except now we disconnect the top port of the second pillar in the third layer, pillar_8, from the arch on the fourth layer, arch_8, to model a *broken* column. We consider the same parameter values as in (100),(101) (and $\mu_{\mathrm{arch}} = (1, 10^{-7})$) except now $\mu_{\mathrm{pillar}_7} = (0.5, 1, 10^{-7})$ to represent a column "stub." We show the displacement field in Figure 14; as expected, the deflections near the broken column are greatly amplified. This example illustrates the ease with which we may consider both parametric and topological variations in design exercises.

ACKNOWLEDGEMENT

This work was supported by OSD/AFOSR/MURI Grant FA9550-09-1-0613 and by the MIT-Singapore International Design Center.

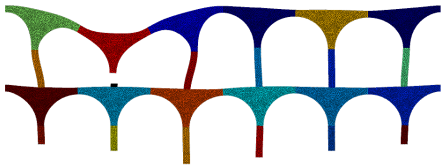

FIGURE 14. Displacement field for the bridge system with one "broken pillar"; the displacement field is scaled by a factor of 10,000.

REFERENCES

[1] H. Antil, M. Heinkenschloss, and R. H. W. Hoppe. Domain decomposition and balanced truncation model reduction for shape optimization of the Stokes system. *Optimization Methods & Software*, 2010. doi: 10.1080/10556781003767904.

[2] H. Antil, M. Heinkenschloss, R. H. W. Hoppe, and D. C. Sorensen. Domain decomposition and model reduction for the numerical solution of PDE constrained optimization problems with localized optimization variables. *Computing and Visualization in Science*, 13(6):249–264, 2010.

[3] M. Barrault, Y. Maday, N. C. Nguyen, and A. T. Patera. An 'empirical interpolation' method: application to efficient reduced-basis discretization of partial differential equations. *Comptes Rendus Mathematique*, 339(9):667–672, 2004.

[4] A. Bermúdez and F. Pena. Galerkin lumped parameter methods for transient problems. *International Journal for Numerical Methods in Engineering*, 86:n/a, doi: 10.1002/nme.3140, 2011.

[5] P. Binev, Cohen A., W. Dahmen, R. DeVore, G. Petrova, and P. Wojtaszczyk. Convergence rates for greedy algorithms in reduced basis methods. Technical report, Aachen Institute for Advanced Study in Computational Engineering Science, Preprint: AICES-2010/05-2, 2010.

[6] P. E. Bjorstad and O. B. Widlund. Iterative methods for the solution of elliptic problems on regions partitioned into substructures. *SIAM Journal on Numerical Analysis*, 23(6):1097–1120, 1986.

[7] S. C. Brenner. The condition number of the Schur complement in domain decompostion. *Numerische Mathematik*, 83:187–203, 1999.

[8] A. Buffa, Y. Maday, A. T. Patera, C. Prud'homme, and G. Turinici. A priori convergence of the greedy algorithm for the parametrized reduced basis. *Mathematical Modelling and Numerical Analysis*, accepted 2010.

[9] Y. Chen, J. S. Hesthaven, and Y. Maday. *A Seamless Reduced Basis Element Methods for 2D Maxwell's Problem: An Introduction*, volume 76. In Spectral and High Order Methods for Partial Differential Equations-Selected papers from the ICASOHOM'09 conference, J Hesthaven and EM Rønquist (eds), 2011.

[10] R. Craig and M. Bampton. Coupling of substructures for dynamic analyses. *AIAA Journal*, 6(7):1313–1319, 1968.

[11] J. L. Eftang, A. T. Patera, and E. M. Rønquist. An "hp" certified reduced basis method for parametrized elliptic partial differential equations. *SIAM Journal on Scientific Computing*, 32(6):3170–3200, 2010.

[12] M. Ganesh, J. S. Hesthaven, and B. Stamm. A reduced basis method for multiple electromagnetic scattering in three dimensions. Technical Report 2011-9, Scientific Computing Group, Brown University, Providence, RI, USA, May 2011.

[13] G. Golub and C. van Loan. *Matrix Computations*. Johns Hopkins University Press, 1996.

[14] D. Gottlieb and S. A. Orszag. *Numerical Analysis of Spectral Methods: Theory and Applications*. SIAM, 1993.

[15] B. Haggblad and L. Eriksson. Model reduction methods for dynamic analyses of large structures. *Computers and Structures*, 47(4-5):735–749, 1993.

[16] W. C. Hurty. On the dynamic analysis of structural systems using component modes. In *First AIAA Annual meeting, Washington, DC*. AIAA paper, no. 64-487, June 29–July 2, 1964.

[17] D.B.P. Huynh, G. Rozza, S. Sen, and A.T. Patera. A successive constraint linear optimization method for lower bounds of parametric coercivity and inf-sup stability constants. *Comptes Rendus Mathematique*, 345(8):473–478, 2007.

[18] E. Isaacson and H. B. Keller. *Computation of Eigenvalues and Eigenvectors, Analysis of Numerical Methods*. Dover, New York, 1994.

[19] B. S. Kirk, J. W. Peterson, R. H. Stogner, and G. F. Carey. `libMesh`: A C++ Library for Parallel Adaptive Mesh Refinement/Coarsening Simulations. *Engineering with Computers*, 22(3–4):237–254, 2006.

[20] D. J. Knezevic and J. W. Peterson. A high-performance parallel implementation of the certified reduced basis method. *Computer Methods in Applied Mechanics and Engineering*, 200(13-16):1455–1466, 2011.

[21] Y. Maday, A. T. Patera, and G. Turinici. A priori convergence theory for reduced-basis approximations of single-parameter elliptic partial differential equations. *Journal of Scientific Computing*, 17:437–446, 2002. 10.1023/A:1015145924517.

[22] Y Maday and EM Rønquist. The reduced basis element method: Application to a thermal fin problem. *SIAM Journal on Scientific Computing*, 26(1):240–258, 2004.

[23] Yvon Maday and Einar M. Rønquist. A reduced-basis element method. *Journal of Scientific Computing*, 17:447–459, 2002. 10.1023/A:1015197908587.

[24] N.C. Nguyen. A multiscale reduced-basis method for parametrized elliptic partial differential equations with multiple scales. *Journal of Computational Physics*, 227:9807–9822, 2007.

[25] C Prud'homme, D Rovas, K Veroy, Y Maday, AT Patera, and G Turinici. Reliable real-time solution of parametrized partial differential equations: Reduced-basis output bounds methods. *Journal of Fluids Engineering*, 124(1):70–80, 2002.

[26] G. Rozza, D. B. P. Huynh, and A. T. Patera. Reduced basis approximation and a posteriori error estimation for affinely parametrized elliptic coercive partial differential equations. *Archives Computational Methods in Engineering*, 15(3):229–275, September 2008.

[27] S. Sen. Reduced basis approximation and *a posteriori* error estimation for many-parameter heat conduction problems. *Numerical Heat Transfer, Part B: Fundamentals*, 54(5):369–389, 2008.

[28] P. Seshu. Substructuring and component mode synthesis. *Shock and Vibration*, 4:199–210, 1997.